DEVELOPMENT OF A MUSCULOSKELETAL MODEL FOR LOAD CARRIAGE

by

Jordan Sturdy

A thesis submitted to the Faculty and the Board of Trustees of the Colorado School of Mines in partial fulfillment of the requirements for the degree of Master of Science (Mechanical Engineering).

Golden, Colorado

Date _____

Signed: _____

Jordan Sturdy

Signed: _____

Dr. Anne Silverman
Thesis Advisor

Golden, Colorado

Date _____

Signed: _____

Dr. John Berger
Professor and Head
Department of Mechanical Engineering

ABSTRACT

Musculoskeletal injury of the lumbar spine and lower extremity is prevalent among military service members, and results in more lost duty days than any other medical condition. Most of these musculoskeletal conditions, such as muscle strains, stress fractures, and joint pain and degradation are attributed to overuse. A key contributor to this overuse is the heavy load service members routinely carry during training and deployment, which is often in excess of recommended maximum weights. Walking with heavy backpack loads causes postural changes and increases the mechanical demand on the musculoskeletal system. In order to alleviate the effects backpack loads on the spine, backpacks are often designed with hip belts in order to redistribute some of the total load from the shoulders and the pelvis. However, it is unknown to what extent the internal forces related to injury risk in the lumbar spine, such as muscle and joint contact forces, are affected by these mitigation strategies.

Therefore, the purpose of this study was to develop a musculoskeletal model incorporating backpack attachment to the torso and pelvis in order to analyze lumbar spine and lower extremity injury risk. Joint contact forces in the lumbar spine and hip were quantified while walking using (1) a shoulder-borne only and (2) a hip-belt assisted backpack design. In addition, robustness of the model was assessed with a probabilistic sensitivity study to investigate the uncertainty in joint contact force estimates due to assumed uncertainty in model parameter values. The results from this work provide novel information regarding injury risk to the lumbar spine related to load carriage. Lumbar spine and hip joint contact forces are greater when walking with backpack loads compared to without. However, implementation of a hip-belt to distribute half of the load from the shoulders to the pelvis does not influence lumbar spine or hip joint contact forces. In addition, backpack attachment parameter values did not substantially effect joint contact force estimates. These results indicate that other factors such as, the total load carried and walking speed, have greater influence on joint contact forces than backpack design. The load carriage model developed will be useful for future analysis of various backpack designs during additional conditions such as sloped walking or running.

TABLE OF CONTENTS

ABSTRACT iii
LIST OF FIGURES v
LIST OF TABLES vi
ACKNOWLEDGEMENTS vii
CHAPTER 1 INTRODUCTION 1
CHAPTER 2 REVIEW OF THE LITERATURE 2
2.1 Walking with Loads 2
2.2 Lower Body 2
2.3 Torso 3
2.5 Backpack Interaction 4
2.4 Musculoskeletal Modeling and Simulation 5
2.5 Summary of Literature 6
CHAPTER 3 MUSCULOSKELETAL MODELING OF LUMBAR SPINE AND HIP JOINT CONTACT FORCES DURING LOAD CARRIAGE WITH DIFFERENT BACKPACK DESIGNS 7
3.1 Abstract 7
3.2 Introduction 7
3.3 Methods 10
3.3.1 Musculoskeletal Model 10
3.3.2 Experimental Data Collection 10
3.3.3 Walking Simulation Development 12
3.3.4 Analysis 13
3.4 Results 14
3.4.1 Simulation Quality 14
3.4.1 Joint Contact Forces 16
3.4.2 Muscle activity 17
3.5 Discussion 19
3.6 Conclusions 21
CHAPTER 4 EVALUATION OF BACKPACK ATTACHMENT PARAMETER UNCERTAINTY ON ESTMATES OF HIP AND LUMBAR SPINE JOINT CONTACT FORCE 22
4.1 Introduction 22
4.2 Methods 22
4.3 Results 23
4.4 Discussion 25
4.4 Conclusion 26
CHAPTER 5 SUMMARY AND CONCLUSIONS 27
REFERENCES 28

LIST OF FIGURES

Figure 3. 1. Representation of the force element interactions for the backpack attachment models. For the shoulder-borne only model (Top) a backpack-torso joint with force elements acting on the vertical and anterior/posterior translational degrees of freedom were defined. For the hip-belt assisted model, an additional backpack-pelvis joint with a force element acting on the vertical translational degree-of-freedom was defined. The total backpack mass and center-of-mass location was identical between models; however, the hip-belt assisted model required two identical and coincident backpack bodies affixed with a weld constraint 11

Figure 3. 2. Average processed electromyographic data (grey shaded region) and corresponding muscle activations from the walking simulations (blue dashed line with error bars) plotted over stance. Time-series data were normalized to the highest value observed during 0L for each muscle and subject 15

Figure 3. 3. Three-dimensional L4-L5 and Hip joint contact forces plotted over stance. 0L: grey shaded region representing the mean ± one standard deviation, SHO: orange dot-dashed line mean with vertical lines indicating ± one standard deviation, HBA: blue dashed line mean with vertical lines indicating ± one standard deviation. Forces were normalized to each participant's bodyweight and then averaged across participants. For L4-L5, the axial force is the compressive force between the two vertebrae, with the anterior and lateral (right side) directions defined positively. Hip joint contact forces between the pelvis and the femur are expressed in the femoral coordinate frame, with positive axial force being the compressive force along the direction of the femur, and anterior and lateral directions defined positively 17

Figure 3. 4. Mean muscle activations (± 1 standard deviation) from the model over the stance phase for each walking condition averaged across participants. 0L – grey shaded region, SHO – orange dotted lines, HBA – blue dashed lines. Activations for each muscle were normalized to the highest value observed in 0L and averaged across participants 18

Figure 4. 1. Probabilistic analysis workflow. Backpack attachment parameter values are modeled as probability distributions. In a 1000 trial Monte-Carlo analysis, the backpack model is defined for each trial (i) using randomly selected values from the input distributions, then a musculoskeletal simulation is performed (ii) using this perturbed model and outcome metrics are extracted (iii) from each iteration to create a probability distribution of each outcome metric. This outcome distribution is then used to compute sensitivity factors attributed to each independent model parameter 23

Figure 4. 2. Cumulative distribution functions (CDF's) of each joint contact force outcome. The baseline value (p=0.5 level) was subtracted from each CDF to center them at 0 and to represent the deviation from baseline rather than overall value of each metric 24

LIST OF TABLES

Table 3. 1. Model muscle groups and their abbreviations. Individual muscles from the model that comprise the group as well as the total number of musculotendon actuators in each muscle group are given. Muscles corresponding to EMG signals are denoted with the superscript “E”. Dominant (right) side muscles were evaluated 13

Table 3. 2. Mean (standard deviation) RMS residual forces and moments applied to the pelvis during right side stance. Forces and moments were normalized to a percent of each participant’s body weight (%BW) and then averaged for each walking condition..... 14

Table 3. 3. Mean (standard deviation) of RMS and maximum kinematic tracking errors for each tracked model coordinate, averaged across participants for each load condition. All coordinates are in degrees except for pelvis mediolateral, anterior, and vertical translation, which are in meters 15

Table 3. 4. Relative amplitude of the motion between the backpack and the torso. The difference between the center-of-mass locations of the backpack and the torso in the global frame was extracted from simulations and 3D marker positions. Amplitudes were calculated as the range of this difference in the vertical and A/P directions. Results from all participants are averaged for both SHO and HBA 16

Table 3. 5. Mean (standard deviation) of average and peak forces in the vertical and anterior/posterior directions reported from the backpack attachment parameters (spring and damper pairs) in N. Only torso attachment parameters are defined for the SHO model, while torso and pelvis attachment parameters are defined for the HBA model. Results from all participants are averaged for each load condition 16

Table 3. 6. Main effects and pairwise comparison results for joint contact force metrics. p-values reported for main effects of backpack and pairwise comparisons between conditions are reported for average forces in L4-L5 and hip during stance (Top) and peak L4-L5 and hip forces during stance. Significant results are in bold..... 18

Table 4. 1. Sensitivity factors for the mean value of each probabilistic model parameter at outcome probability levels 0.1, 0.5, and 0.9 as well as the average sensitivity factor from the entire distribution. Parameters with the greatest influence on an outcome metric are bolded 25

ACKNOWLEDGEMENTS

I would like to thank my advisor, Dr. Anne Silverman, for her support and guidance throughout this research process and my graduate career. I would also like to thank my committee members, Dr. Pinata Sessoms, and Dr. Jeff Ackerman, for their guidance and personal investment in support of my thesis. The support of all members of the Functional Biomechanics Laboratory at Mines has been essential in pursuit of my thesis, and I have greatly improved as a researcher because of them. Most importantly, I would like to thank my family for their love and support as I pursue my long term goals.

DISCLAIMER: I am an employee of the U.S. Government. This work was prepared as part of my official duties. Title 17, U.S.C. §105 provides that copyright protection under this title is not available for any work of the U.S. Government. Title 17, U.S.C. §101 defines a U.S. Government work as work prepared by a military service member or employee of the U.S. Government as part of that person's official duties. The views expressed in this article are those of the authors and do not necessarily reflect the official policy or position of the Department of the Navy, Department of Defense, nor the U.S. Government. The study protocol was approved by the Naval Health Research Center Institutional Review Board in compliance with all applicable Federal regulations governing the protection of human subjects. Research data were derived from an approved Naval Health Research Center Institutional Review Board protocol number NHRC.2013.0022. This work was supported by the U.S. Defense Health Agency Military Operational Medicine Research Program work unit no. N1814 and Office of Naval Research work unit no. N1504

CHAPTER 1

INTRODUCTION

Military service members encounter a wide variety of environment, terrain and physical requirements, which require varying movement and muscle activation patterns. For example, steep uphill or downhill slopes and heavy (> 30 kilogram) carried loads are commonly encountered during training and deployment. Non-combat musculoskeletal injuries are a substantial problem among military service members with up to 75% of all hospitalizations due to disease and non-battle injury, half of which are musculoskeletal (Belmont Jr. et al., 2010) and are often attributed to overuse (Hauret et al., 2010). In addition, injuries to the lumbar spine comprised 20% of all musculoskeletal injuries related to overuse (Hauret et al., 2010). Detailed biomechanical analyses are critical for understanding the mechanical stresses placed upon the structural tissues. However, many relevant *in vivo* quantities are difficult or impossible to measure directly.

Computational modeling and simulation techniques can be used to estimate muscle forces and joint contact forces (e.g., Piazza, 2006; Zajac et al., 2003) such as the compressive forces in the lumbar spine during activities of daily living (e.g., Actis et al., 2018b; Yoder et al., 2015). In addition, models incorporating backpack loads have been used to predict adaptation of lower-limb muscles (Dorn et al., 2015) and estimate knee joint loads during dynamic tasks (Ramsay et al., 2016). However, these load carriage models have simplified representations of backpack-human interactions and torso kinematics, which are likely insufficient for accurate estimates of trunk muscle and joint forces.

In this research, a musculoskeletal model of the trunk and lower limbs that incorporates spinal rhythm to describe lumbar joint rotations and robust backpack attachments capable of distributing load between the shoulders and hips was developed. This model is needed to quantify joint contact and muscle forces in the lower limbs and lumbar spine during load carriage. I combined a full body model (Actis et al., 2018a) with backpack interactions (e.g., Foissac et al., 2009; Ramsay et al., 2016; Selk Ghafari et al., 2010). With this model, I developed musculoskeletal simulations of walking with and without load on level as well as sloped surfaces. To validate this model, I compared experimentally measured muscle excitations (electromyography) to estimated activation patterns from the simulations for each walking condition. In addition, I quantified the effect of backpack attachment parameter uncertainty on joint contact force estimates. This work will facilitate further development of backpack interaction models to evaluate backpack performance across a range of walking slopes and will provide insight into overuse injuries in military service members.

CHAPTER 2

REVIEW OF THE LITERATURE

A review of the literature regarding the biomechanical characteristics of walking with backpack load carriage, as well as the current state of modeling and simulation techniques is provided in this chapter.

2.1 Walking with Loads

The neuromusculoskeletal system adapts to carrying heavy loads, evidenced by differences in kinematics, kinetics, and muscle activity compared to unloaded walking. These biomechanical adaptations may be a strategy to support greater body mass and/or to maintain balance by keeping the body center of mass (COM) over the base of support. There is substantial prior work investigating lower body biomechanics during loaded walking compared to unloaded walking. However, while there are also studies regarding trunk, or torso, biomechanics during loaded walking, the results are limited by simplification of spinal motion and/or a small number of back and abdomen muscles included in the analyses. Musculoskeletal modeling and simulation has been increasingly used to study lower body biomechanics during loaded walking and running (Dorn et al., 2015; Lenton et al., 2018a; Ramsay et al., 2016). However, the models used have thus far utilized simplified representations of spinal kinematics and/or backpack interactions, and a greater level of detail is needed to quantify relevant lumbar joint contact forces and back and abdominal muscle forces. Therefore, the goal of this research was to develop a full body, musculoskeletal model that incorporates lumbar spine motion and realistic backpack attachments that estimate muscle excitations that are similar to signals reported in the literature under similar walking conditions.

2.2 Lower Body

Lower body biomechanical changes due to load carriage are reflective of the increased mechanical demand in an effort to support and balance a greater total mass. For example, the ankle, knee, and hip are all more flexed at heel strike and more extended in late stance while carrying a load, resulting in greater hip and ankle ranges-of-motion over the gait cycle and knee range-of-motion during stance (Attwells et al., 2006; Seay et al., 2014; Wang et al., 2013). However, the maximum knee flexion during swing decreased with loads of more than 20% body weight (Ghori and Luckwill, 1985), resulting in an overall decreased range-of-motion (Harman et al., 1999). To support the carried load, net joint moments at the hip, knee, and ankle are all significantly greater compared to unloaded walking (Krupenevich et al., 2015; Seay et al., 2014). However, joint moments are likely dependent on the amount of load carried. For example, when the carried load was less than 22 kilograms, there were greater hip flexion, early stance knee flexion and extension, and ankle plantarflexion moments, yet no changes for hip extension, late stance knee flexion, and ankle dorsiflexion moments compared to unloaded walking (Krupenevich et al., 2015; Seay et al., 2014). When loads greater than 32 kilograms have been carried, all peak flexion and extension moments were greater than unloaded walking (Seay et al., 2014; Wang et al., 2013). Further, one study found that the knee extension moment was disproportionately increased compared to the ankle and hip moments. When total mass (body plus backpack) increased by 49%, the ankle peak plantar-flexion moment increased 28%, hip peak extension moment increased by 47%, and knee peak extension moment increased by 98%, which suggests heavy reliance on the quadriceps muscles for load carriage (Harman et al., 2000). Similarly, ground reaction forces are greater when

walking with load. One study found that peak, average, and impulsive forces for the vertical, braking, propulsive, and medial directions were all greater as the carried load increased from 6 up to 47 kilograms while the lateral direction remained unchanged (Harman et al., 2000). In addition, power generation in late-stance is greater at the hip and ankle joints while walking with load compared to unloaded (Krupenevich et al., 2015). Power absorption at the knee is greater when walking with load compared to unloaded (Krupenevich et al., 2015; Wang et al., 2013). These increased lower body joint power requirements when walking with a backpack load suggest greater activity from the muscles spanning each joint. This is further evidenced by the knee absorbing more power with increased load while the duration of activity from the vastus lateralis is also increased (Ghori and Luckwill, 1985). However, the duration of activity in the semitendinosus/semimembranosus is not different from level walking (Ghori and Luckwill, 1985). Average activation amplitude of the rectus femoris and gastrocnemius is greater during loaded compared to unloaded walking, while biceps femoris long head and tibialis anterior amplitudes remain unchanged between loaded and unloaded walking (Harman et al., 2000).

In summary, loaded walking results in substantial kinematic differences and greater magnitudes of joint moments and powers in the lower body compared to unloaded walking. However, the effect of added load may not be evenly distributed among the lower limb joints, as the knee moments are increased disproportionately more than the ankle and hip.

2.3 Torso

Postural adaptations at the trunk while carrying load position the backpack plus body COM over the feet (Muslim and Nussbaum, 2016a). A more forward tilted trunk and pelvis are consistent postural adjustments made when loads are carried posteriorly, such as with a backpack. Mean and peak torso angle increase progressively with load (Goh et al., 1998; Muslim and Nussbaum, 2016a), and pelvic anterior tilt at heel strike is greater (Wang et al., 2013) with posteriorly carried loads compared to unloaded walking. However, trunk range-of-motion in the sagittal plane is similar between loaded and unloaded walking, suggesting the primary response of the trunk is to reposition the body COM (Attwells et al., 2006). In one study, the change in trunk angle between loaded and unloaded walking was found to be greater for female subjects than it was for male subjects (Krupenevich et al., 2015). However, this effect may be due to body size as both groups carried the same fixed load, and the female group was on average shorter and lighter than the male group. To control the motion of the additional carried load, mean and peak moment about the lumbosacral (L5S1) joint increased with the mass of the load (Muslim and Nussbaum, 2016a). A greater lumbosacral moment suggests a change in trunk muscle activity, which plays a critical role in providing spinal stability to maintain equilibrium (Granata and Orishimo, 2001; Lee et al., 2006). However, at certain loads, there is a decrease in muscle activity, which suggests a load mass threshold between 30 and 40-kg, above which activity from erector spinae is greater than unloaded walking (Knapik et al., 1996). For example, when 20-kg backpack loads were carried, a lower activation of erector spinae was found compared to carrying no load (Bobet and Norman, 1984). People may regulate balance in a fundamentally different way during load carriage, indicated by a more posterior position of the trunk-plus-load COM during loaded compared to unloaded walking, which reduces the net extensor torque requirement compared to keeping the COM position unchanged (Harman et al., 2000; Knapik et al., 1996). At low loads, this reduced extensor moment lessened erector spinae activity, but may have increased the abdominal

muscle activity to prevent backward rotation of the trunk (Harman et al., 2000). As erector spinae activity decreased with loads up to 15% body weight, greater activity from rectus abdominus and external oblique muscles was required to maintain posture (Devroey et al., 2007). However, erector spinae activity increased when loads above 20-kg were used, and one study found a significant load effect on erector spinae activity for progressive loads from 20-47 kg (Harman et al., 2000). Further, when carrying loads greater than 35% body weight, muscle activity from erector spinae, rectus abdominus, and external obliques all increased compared to lighter or no load (Muslim and Nussbaum, 2016a). Together, this body of work suggests non-linear responses of the erector spinae to walking with an added load.

In summary, the primary torso adaptation to walking with carried loads is a change in sagittal angle to position the COM over the base of support. While the kinematic changes between unloaded walking and loaded walking are consistent, changes in muscle activation are likely nonlinear due to the posterior shift in position of the body COM during loaded walking.

2.5 Backpack Interaction

Movement of a backpack load results in an externally applied force to the musculoskeletal system. Various modeling and experimental approaches have been used to study this interaction between the backpack and the human as it relates to a variety of metrics such as stability and intersegmental forces (e.g., Ackerman et al., 2017; Foissac et al., 2009; LaFiandra and Harman, 2004; Goh et al., 1998; Ren et al., 2005a). During walking, the vertical force applied by the backpack to the body was increased proportionally greater to the increased mass of the load (LaFiandra and Harman, 2004). Further, this external force will affect the internal joint forces, which have been estimated at the lumbosacral joint using inverse dynamics and found 26.7% and 64% greater intersegmental forces in response to carrying 15% and 30% body weight compared to no load (Goh et al., 1998). These findings demonstrate that differences in intersegmental forces are not be proportional to the change in external loads.

Load distribution systems that transfer a portion of the total carried mass from the shoulders to the pelvis have recently been investigated for their effect on lower limb quantities (e.g. Lenton et al., 2018a, 2018b, 2018c). While these studies focused on body armor loads and not backpack loads, the usage of various hip belt implementations did not influence knee joint contact loads (Lenton et al., 2018a). However, differences in postural adaptations were found with less trunk flexion while using a hip belt compared to shoulder borne for 15 kg but not for 30 kg loads (Lenton et al., 2018c). In addition, hip abduction moment was lower while using a hip belt compared to shoulder borne for 30 kg but not for 15 kg loads (Lenton et al., 2018c).

In summary, backpack attachment design has an effect on the external moment that is balanced out by the lumbar spine and hip joint moments during walking. These differences will cause changes in the muscle forces required to produce net joint moments. Quantification of joint contact forces, which are larger than the joint intersegmental forces because they include these muscular contributions, in the low back is important for understanding injuries resulting from load carriage. Little is known about the response of erector spinae, rectus abdominus, and external oblique muscles to walking while carrying loads and with different load distributions.

2.4 Musculoskeletal Modeling and Simulation

Internal forces such as those in muscles and tendons or the contact forces between joint surfaces are important metrics to quantify potential mechanisms of injury, yet measurement of these forces *in vivo* requires invasive procedures (e.g., Wilke et al., 1999). In addition, muscle forces are large contributors to joint contact forces, although these contributions are not present in the calculation of intersegmental forces using inverse dynamics approaches (Sasaki and Neptune, 2010). Traditional inverse dynamics and electromyographic analyses can reveal variations in net joint moments and muscle activation patterns and are often used in clinical diagnosis and prescription (e.g., Piazza, 2006; Sutherland, 2001). While electromyography can provide information regarding whether a muscle is active or not, it does not provide estimates of muscle force. Further, these analyses cannot establish causal relationships between muscle action and the resulting kinematics and kinetics of movement because many different muscle activation patterns could produce the same movement at a single joint due to the redundant nature of the musculoskeletal system (Zajac et al., 2002). In addition, muscles affect loads and motions at joints they do not span due to dynamic coupling of the musculoskeletal system (Piazza, 2006; Zajac et al., 2002). In contrast, computational modeling and simulation approaches can be used to estimate these forces (Piazza, 2006). For example, static optimization approaches minimize a cost function (such as instantaneous metabolic power, muscle stress, or the sum of squared muscle activations) at every time step to compute the muscle activations required to produce the net joint moment determined by inverse dynamics (Anderson and Pandy, 2001a). These optimization results can then be used to calculate the total joint contact force as the sum of the total force generated by the muscles spanning the joint and the intersegmental force computed using inverse dynamics (Sasaki and Neptune, 2010; Yoder et al., 2015; Zajac et al., 2002).

To quantify muscle and joint contact forces in the lumbar spine, models must account for the multi-segmented motion of the low back. However, most musculoskeletal models have used a single rigid body to represent the head, arms, trunk and sometimes pelvis. While these models are sufficient for analyses regarding the lower body, they clearly have limitations when applied to upper body analyses. Recent musculoskeletal models have incorporated detailed representations of the torso (Actis et al., 2018a; Bassani et al., 2017; Christophy et al., 2012; Yoder et al., 2015), and have been used to study low back mechanics among lower limb amputees who have asymmetric movement patterns (Actis et al., 2018b; Yoder et al., 2015). However, when new models are created, confidence in simulation outputs is dependent on whether model validation can be performed via relevant *in vivo* information from a similar movement (Hicks et al., 2015). Joint contact forces from a lumbar spine model have been validated during multiple movements, including four conditions wherein a 20kg load was lifted, against *in vivo* intradiscal pressure measurements (Bassani et al., 2017). A similar full body model having 19 independent degrees of freedom with five lumbar joint motions defined relative to trunk-pelvis motion has produced simulations to predict joint contact forces during trunk range-of-motion movements that were validated with experimental *in vivo* intradiscal pressure measurements (Actis et al., 2018a). This model was also used to quantify differences in lumbar joint contact forces between lower limb amputees and non-amputee controls during a sit to stand motion (Actis et al., 2018b).

Simulation studies involving backpack load carriage predominantly model the backpack as a point mass with a rigid or stiff attachment to the torso offset by a fixed distance posterior to the torso (Dorn et al., 2015; Ramsay et al., 2016). In some cases the backpack slides axially along the torso, but is otherwise constrained to move with the trunk (e.g., Selk Ghafari et al., 2010). Using these modeling assumptions, static optimization was used to estimate muscle forces and quantify knee joint contact force during a run-to-stop maneuver while carrying increasing backpack loads (Ramsay et al., 2016). Forward dynamic simulations using this backpack interaction model predicted distinct patterns of leg muscle mechanical power distribution to the trunk, ipsilateral, and contralateral legs when carrying load compared to unloaded walking (Selk Ghafari et al., 2010). However, the interaction between the backpack and torso can be modeled with greater complexity, which can better inform backpack design and identify mechanisms of musculoskeletal injury. In the sagittal plane alone, dynamic equations-of-motion account for relative axial, anterior, and angular motion between the mass centers of the load and torso (e.g., Ren et al., 2005). Redundancy in the suspension interface and nonlinear stiffness and damping properties at the attachment points further complicate the pack-torso interaction and biomechanical response of the musculoskeletal system in response to backpack attachments (Ren et al., 2005).

In summary, quantification of muscle and joint contact forces is important for understanding potential injury mechanisms due to the stresses placed upon joints and tissues. Without optimization through computational modeling and simulation, these internal forces would be impossible to estimate during dynamic tasks such as load carriage. Recent work has demonstrated the success of using modeling and simulation approaches to quantify lumbar joint contact forces during various tasks. In addition, these computational methods have also been used to estimate lower limb quantities such as muscular power distribution and joint contact force during load carriage. However, current load carriage models are extremely simplified, and are not suitable for estimating muscle and joint contact forces in the spine.

2.5 Summary of Literature

Substantial kinetic, kinematic, and muscular changes are made in response to walking while carrying posterior loads, and these biomechanical changes are well understood for the lower body. However, while there are well documented postural changes made at the trunk during loaded walking, very little is known about the muscular response of the trunk to walking with posterior loads. In addition, the effects of load distribution between the torso and pelvis on back and abdomen muscle activity is unknown. These muscular responses are important to understanding internal joint loads which can be estimated through musculoskeletal modeling and simulation approaches. However, existing musculoskeletal models that incorporate a backpack are unsuitable for quantifying trunk and abdominal muscle forces and joint contact forces in the lumbar spine. Therefore, the goal of this work was to develop a musculoskeletal model for load carriage simulations to quantify these internal forces for greater understanding of potential long-term injury risk.

CHAPTER 3

MUSCULOSKELETAL MODELING OF LUMBAR SPINE AND HIP JOINT CONTACT FORCES DURING LOAD CARRIAGE WITH DIFFERENT BACKPACK DESIGNS

A paper to be submitted to the *Journal of Biomechanics*

Jordan T. Sturdy[1], Pinata H. Sessoms[2], and Anne K. Silverman[3]

3.1 Abstract

Musculoskeletal injuries of the lumbar spine and lower extremity are common among Military service members who are required to carry heavy loads. However, the underlying biomechanics that may contribute to injury risk are unclear. Quantifying muscle and joint contact forces through musculoskeletal modeling and simulation is important for evaluating potential long-term injury risk in this population. Further, different military backpack designs likely influence the biomechanics of load carriage and these internal forces, but these designs are rarely evaluated biomechanically, especially in relation to lumbar and hip joint contact forces. To evaluate the biomechanics of walking with different backpack designs, kinematic, ground reaction force, and electromyographic data were collected from six US Marines while walking without load, with a traditional military backpack with shoulder straps, and with a distributed load system incorporating a hip belt with a flexible spine. A musculoskeletal model was developed with multiple backpack attachments modeled with spring and damper attachments between the backpack and the wearer at the (1) shoulders or (2) shoulders and pelvis. This model incorporating the lumbar spine and 294 muscles in the trunk and low back was developed and used to estimate muscle and joint contact forces in each loading configuration. Carrying loads increased average L4-L5 force compared to unloaded walking by 52.8% and 41.5% during shoulder only and shoulder and pelvis backpack configurations respectively. Hip joint contact forces were also greater during shoulder only and shoulder and pelvis backpack configurations compared to unloaded walking in both axial (34.3% and 25.0%) and A/P (28.6% and 32.4%) directions. However, there were no differences in contact forces between the two backpack designs, suggesting that these quantities are not significantly influenced by how the backpack is attached to the body. Future research incorporating standardized walking speeds and additional participants is suggested for further evaluation of different backpack configurations.

3.2 Introduction

Musculoskeletal injury is prevalent among US Military service members, with up to 50% of active duty personnel sustaining such an injury each year (U.S. Army Public Health Center, 2017). Even during heavy periods of Military engagement, non-combat related musculoskeletal injury remains the largest casualty category resulting

---

[1] Master's candidate in Mechanical Engineering at Colorado School of Mines in Golden, CO. Primary author responsible for model development, data analysis, results interpretation, and manuscript preparation.

[2] Director of Physical and Cognitive Research Environment laboratory at Naval Health Research Center in San Diego, CA. Responsible for study design, supervised data collection and participant recruitment, assisted with manuscript revision.

[3] Associate Professor of Mechanical Engineering at Colorado School of Mines in Golden, CO. Research advisor to primary author, involved with model development, results interpretation, and manuscript preparation.

in lost duty days or medical evacuation for active service members (Belmont Jr. et al., 2010). Musculoskeletal injuries are often attributed to overuse due to the demanding physical requirements related to training and occupational tasks (Hauret et al., 2010; Schuh et al., 2017). For example, Marine assault loads range from 97 to 135 lbs, or more than double the recommended maximum of 51 lbs (Bachkosky et al., 2007). Carrying these heavy loads may be related to the high rates of musculoskeletal injury, specifically low back pain and spine injury, among service members. The back and spine are the most common location of musculoskeletal injury (Armed Forces Health Surveillance Branch, 2017), with many of these cases affecting the lumbar spine (Hauret et al., 2010). The lower extremity as a whole suffers similar injury rates as the back and spine; however, the hip sustains the fewest number of injuries of the lower extremity (Hauret et al., 2010).

Backpack dynamics likely influence spinal loads and with implications for musculoskeletal injury, as they produce reaction forces at their points of attachment to the body (LaFiandra and Harman, 2004). Relative motion between the backpack and torso are influenced by the stiffness and damping properties of attachments (Ackerman et al., 2017; Foissac et al., 2009), and these properties will determine the reaction forces between backpack and body (Ren et al., 2005). Recent work using musculoskeletal modeling and simulation for load carriage has focused on lower extremity metrics rather than the lumbar spine (e.g., Lenton et al., 2018; Ramsay, Hancock, O'Donovan, & Brown, 2016). Thus, it is not surprising that detailed load interactions between the backpack and body have not been developed in a comprehensive musculoskeletal model. In addition, muscles must produce force to balance the external forces and moments such as those created by a backpack in order to maintain postural control (Bobet and Norman, 1984; Devroey et al., 2007). Backpacks are often designed with hip belts to reduce the amount of load on the shoulders, which may reduce injury in the back as a portion of the carried load is transmitted to the pelvis (Knapik et al., 1996). Transference of load from the shoulders onto the hips effectively brings the backpack load closer to the body's center-of-mass (Stevenson et al., 2000), which reduces the net back extensor moment imposed by the backpack and the forward trunk lean that is required to maintain balance (Bobet and Norman, 1984; Goh et al., 1998). Various methods of distributing the carried load have been explored including implementation of body armor with a hip belt (Lenton et al., 2018b) and carrying a portion of the load anteriorly (Seay et al., 2014), yet large backpacks remain the method of carrying marching loads up to 60 kg. Further, while implementation of hip-belts is widely believed to reduce discomfort and injury at the shoulders and upper back, it is unknown how this method of load distribution effects internal forces of the lower back and hip.

Detailed analyses of these internal muscle and joint forces, and their loading rates are important for understanding the mechanisms related to musculoskeletal injury. That is, excessive loads and loading rates have been associated with both acute and chronic injury (Milgrom, 2001; Schache et al., 2010). However, direct *in vivo* measurement of these internal forces is difficult or impossible to perform in most studies because it requires invasive procedures that can be painful, costly, and may damage the integrity of joint tissue (Wilke et al., 1999). Because of these concerns, reported *in vivo* joint loads are often measured from instrumented joint prostheses, which may not reflect biological joint loads (e.g, Hodge et al., 1986; Kutzner et al., 2010) and/or only include one or two people in the analysis (e.g., Hodge et al., 1986; Wilke et al., 2001, 1999). For example, measurements of intra-discal pressure during a variety of activities have been taken by inserting a pressure transducer into the disc between the 4^{th} and 5^{th}

lumbar vertebrae (Wilke et al., 2001, 1999). In contrast to direct *in vivo* measurement, musculoskeletal modeling and simulation approaches can be used to estimate muscle and joint contact forces (e.g., Piazza, 2006; Zajac et al., 2003), such as the compressive forces in the lumbar spine during activities of daily living (e.g., Actis et al., 2018b; Yoder et al., 2015) and knee joint loads during dynamic tasks (e.g., Ramsay et al., 2016; Sasaki and Neptune, 2010; Silverman and Neptune, 2014). Recently, detailed musculoskeletal models of the lumbar spine have been developed (e.g., Bruno et al., 2015; Christophy et al., 2012) to include realistic musculature and incorporate lumbopelvic rhythm, which affects estimates of lumbar joint contact force (Tafazzol et al., 2014). Full body models have combined these detailed spine models with established lower body models to facilitate investigation of spinal loads during activities of daily living (Actis et al., 2018b; Bassani et al., 2017; Raabe and Chaudhari, 2016). However, these models have not been applied to analyze load carriage.

Muscle activation, which is related to muscle force, can be measured non-invasively and is useful for validation of musculoskeletal models and simulations. Greater lower limb muscle activity has been well documented in the vastii, rectus femoris, and gastrocnemius during loaded compared to unloaded walking (Ghori and Luckwill, 1985; Harman et al., 2000; Paul et al., 2016). While greater muscle activity in the lower limb may be expected during load carriage compared to unloaded walking as the total mass that needs to be accelerated is greater, muscle activity patterns in the low back and abdomen are not greater with all loads. For example, activation in the lumbar paraspinals is smaller during loaded compared to unloaded standing (Devroey et al., 2007) and walking (Bobet and Norman, 1984; Harman et al., 2000) when the weight of the backpack is small (less than 15% body weight or 20 kg), but the activation of these muscles increases during walking as loads increase from 20 to 47 kg (Harman et al., 2000). In addition, abdominal muscles have greater activation during loaded standing (Devroey et al., 2007) and walking (Muslim and Nussbaum, 2016b) compared to unloaded conditions. These varied results illustrate the complex interaction between backpack loads and the muscle activity that directly affects joint contact forces. Further, muscle responses to altered backpack configurations has not been investigated.

Therefore, the purpose of this study was to develop a full body musculoskeletal model including a backpack with multiple attachment points to quantify lumbar and lower extremity muscle and joint contact forces. We hypothesized that a hip-belt assisted load carriage design that reduces the amount of load borne at the shoulders would require less muscle activity from the paraspinals and abdomen, resulting in a lower lumbar joint contact force compared to a shoulder-borne design. Further, we hypothesized that the hip joint contact force would be lower with a hip-belt assisted compared to shoulder-borne design due to reduced required hip moment from the hip extensor muscles to counteract the external moment of the backpack on the person. In addition, we expect less muscle activation from the gluteus maximus and hamstrings during hip-belt assisted load carriage compared to shoulder-borne. However, because the total mass above the pelvis will remain the same in either backpack design, no differences are expected in rectus femoris activation, which contributes to forward acceleration of the trunk and pelvis (Neptune et al., 2008).

3.3 Methods

3.3.1 Musculoskeletal Model

A full body load carriage model with backpack attachment parameters was developed in OpenSim v3.3 (simtk.org) using a baseline model that was previously validated for L4-L5 contact load prediction during trunk-pelvis range of motion tasks (Actis et al., 2018a). This model, also developed in OpenSim 3.3 (Anderson and Pandy, 2001b, 1999; Delp et al., 2007, 1990; Yamaguchi and Zajac, 1989), consists of 294 Hill-type musculotendon actuators with force-length-velocity properties (Zajac, 1989) and 19 independent degrees of freedom to describe the lower extremities, pelvis, and torso, with detail of the lumbar spine motion relative to torso-pelvis motion (Christophy et al., 2012). Muscle strengths for the base model were tuned to represent a young, active population using magnetic resonance imaging data from 24 subjects and cadaveric data from 21 subjects (Rajagopal et al., 2016).

Two models were created to represent shoulder-borne only and hip-belt assisted load carriage. Joints between the backpack and the musculoskeletal system were defined to represent attachment to the torso as well as the pelvis (hip-belt assisted model only). Passive linear springs were implemented on the vertical translational degrees of freedom of the backpack-torso and backpack-pelvis joints as well as the anterior/posterior translational degree-of-freedom of the backpack-torso joint (Figure 3. 1). The backpack-torso joint was defined at the torso center-of-mass, and backpack center-of-mass location was 0.135 meters posterior and 0.0475 meters inferior to the backpack-torso joint such that the load is packed close to the back and similar in height to the torso center-of-mass (Hinrichs et al., 1982; LaFiandra and Harman, 2004; Pelot et al., 2000). Addition of a backpack-pelvis joint creates a closed loop between the backpack and the wearer; however, OpenSim requires that the hierarchy of bodies is represented as a tree (i.e., each body has a single joint leading toward the pelvis). Thus, in order to implement a closed loop system, the backpack body was split into two identical and coincident bodies, fixed together with a weld constraint, each with half the mass and inertia as the original backpack body. The backpack-pelvis joint was defined 0.1 m superior and 0.15 m posterior to the pelvic origin, and the relative location of the pelvis backpack body was offset from the joint location such that its center-of-mass location corresponded with that of the shoulder backpack body in the default pose. Each translational attachment force (F_{DoF}) was given by Equation 3. 1:

$$F_{DoF} = k * q_{DoF} + M_{pack} * \ddot{q}_{DoF} + c * \dot{q}_{DoF} \quad (3.1)$$

where q_{DoF} is the horizontal or vertical backpack-torso joint motion or vertical backpack-pelvis joint motion, M_{pack} is the mass of the backpack, k is the spring constant, and c is the damping coefficient. Further, k and c were uniformly defined for all attachment parameters as $5060\ Nm^{-1}$ and $320\ Nsm^{-1}$, respectively (Foissac et al., 2009).

3.3.2 Experimental Data Collection

Kinematic, ground reaction force and electromyographic data were previously collected from active duty U.S. Marines (6 males, 27.17±3.97 years; 1.81±0.04 m; 87.17±8.05 kg) during walking at self-selected speeds with and without load and wearing two different backpack designs (shoulder-borne – SHO, and hip-belt assisted – HBA). All participants provided written informed consent for the protocol approved by the institutional review board.

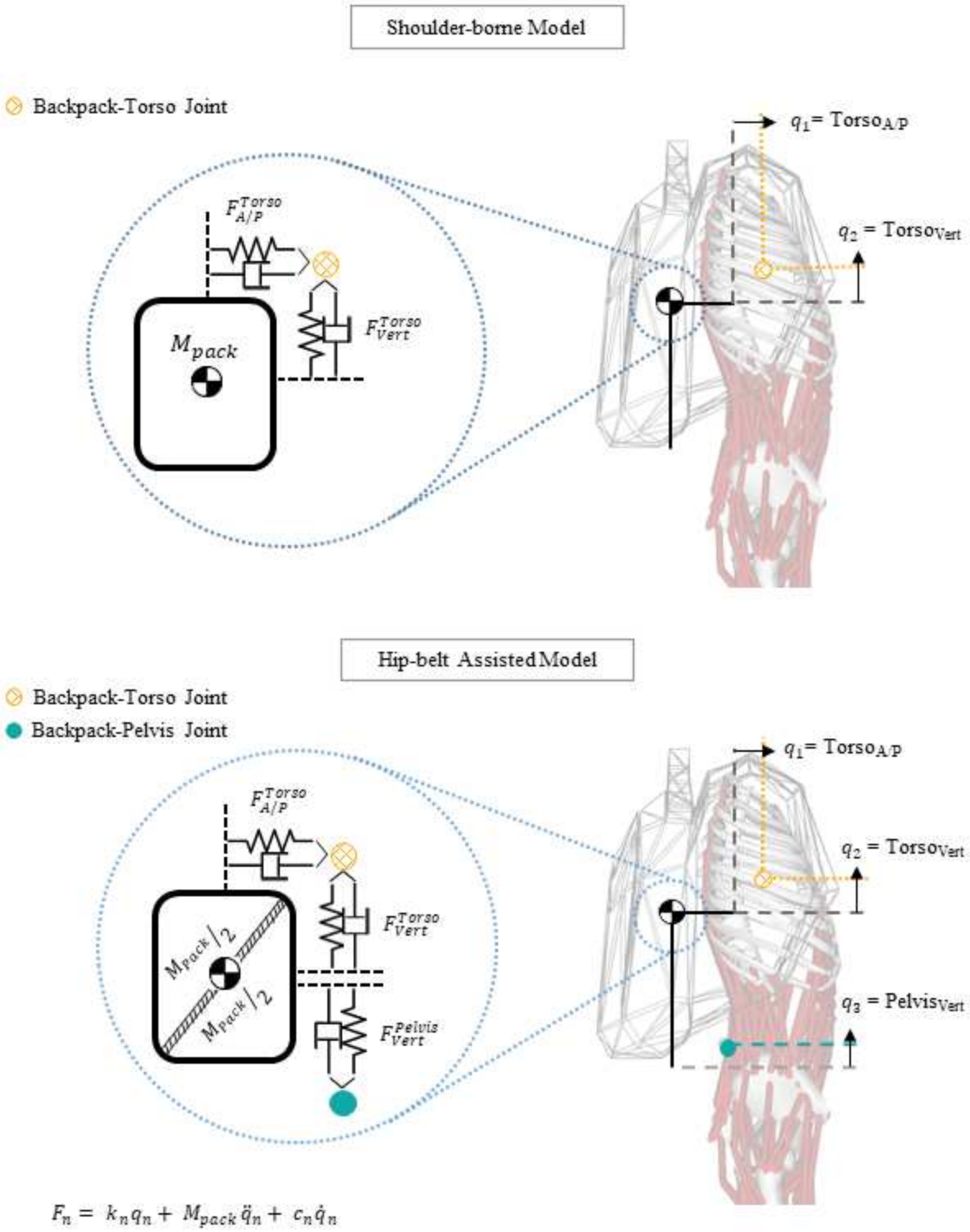

Figure 3. 1. Representation of the force element interactions for the backpack attachment models. For the shoulder-borne only model (Top) a backpack-torso joint with force elements acting on the vertical and anterior/posterior translational degrees of freedom were defined. For the hip-belt assisted model, an additional backpack-pelvis joint with a force element acting on the vertical translational degree-of-freedom was defined. The total backpack mass and center-of-mass location was identical between models; however, the hip-belt assisted model required two identical and coincident backpack bodies affixed with a weld constraint.

During the loaded conditions, participants wore standard body armor (~15 kg) as well as a weighted standard backpack resulting in a total added load of 38.56±0.83 kg. Kinematic data were collected in multiple 30 second recordings at 120 Hz from an optical motion capture system with 14 cameras (Motion Analysis Corp. Santa Rosa, CA). A set of 53 retroreflective markers were used to track whole body motion with marker clusters placed on the thighs and shanks (Collins et al., 2009). An additional three markers were placed on the top, and left and right sides of the backpack during loaded conditions. Ankle, knee, and hip joint centers were computed from the marker clusters using a functional joint definition (Schwartz and Rozumalski, 2005). Three-dimensional ground reaction forces were recorded at 1200 Hz from each foot using an instrumented treadmill (Motek-Forcelink, Amsterdam, Netherlands). Muscle activity was also collected at 1200 Hz using surface electromyography (EMG) sensors (Delsys, Boston, MA) from the dominant-side erector spinae (ES), vastus medialis (VAS), and gastrocnemius (GAS).

3.3.3 Walking Simulation Development

Walking simulations were generated in OpenSim 3.3 using kinematics and ground reaction forcess from the experimental data collection. First, uniform scale factors of each body segment were computed based on marker position during a static standing trial for each participant. To represent the effect of body armor worn on the torso, approximately 15 kg was added to the mass of each participant's scaled torso body in the SHO and HBA models. Because the backpacks used and loads carried were consistent for all participants, the backpack body was not scaled. Muscle strengths for each participant were scaled based on a mass-length scaling law that multiplied the generic maximum isometric force of each muscle by the ratio of scaled body mass to generic mass, and generic to scaled musculotendon length (Correa and Pandy, 2011). Joint definitions for the backpack attachment model were changed to reflect the load condition. Only the backpack-torso joint was defined during SHO, while the backpack-torso and backpack-pelvis joints were both defined during HBA. Unloaded walking did not have a backpack or its associated attachments. Then, an inverse kinematics solution was determined from the experimentally measured marker trajectories using an eight segment model with 19 degrees of freedom for each walking trial using a least squares optimization algorithm (Lu and O'Connor, 1999) in Visual3D (C-motion, Inc., Germantown, MD). We performed a residual reduction algorithm (RRA) (Delp et al., 2007) in OpenSim to adjust model mass, torso center-of-mass location, and the inverse kinematics solution to improve dynamic consistency. Motion of the backpack was not tracked during simulations from the inverse kinematics solution and was created as the result of the model attachment definitions and the pelvis and/or torso motion. A static optimization algorithm was then used to solve the muscle recruitment problem to resolve the required net joint moments into individual muscle forces at each instant of the gait cycle. The sum of cubed muscle activations was minimized at each time step (Equation 3. 2).

$$Minimize:\ J = \sum_{m=1}^{n} (a_m)^3 \tag{3.2}$$

subject to the following constraint (Equation 3. 3) at each joint:

$$\sum_{m=1}^{n} [a_m f(F_m^0, l_m, v_m)] r_{mj} = \tau_j \tag{3.3}$$

where: a_m is the activation level from 0 to 1 of muscle m, the maximum force of a muscle (f) is a function of a muscle's maximum isometric force (F_m^0), length (l_m), and contractile velocity (v_m), and r_{mj} is the moment arm of muscle m about joint j, and τ_j is the net torque about joint j. In static optimization, an inextensible tendon is assumed and the passive properties of the parallel elastic element are not considered, and thus the active muscle fiber force is computed. Using these estimated muscle forces, we performed a joint reaction analysis to calculate three-dimensional joint contact forces between the 4th and 5th lumbar vertebrae in the 5th vertebrae reference frame (L4-L5) and between the pelvis and femur in the femur reference frame (Hip) in each walking condition. Axial L4-L5 and hip forces were inverted such that compressive forces were defined positively, anterior/posterior (A/P) and medial/lateral (M/L) forces were positive in the anterior and lateral (right for L4-L5) directions respectively.

3.3.4 Analysis

Kinematic and ground reaction force data were filtered using a 4th-order, bi-directional low-pass Butterworth filter with a 6 Hz cutoff frequency and were inputs to the simulations. EMG data were band-pass filtered between 60 and 400 Hz, demeaned, and full-wave rectified and were used to validate model activations. A 10 Hz low-pass filter was applied to the rectified EMG signal. EMG data were processed and analyzed for 10 dominant-side (right) leg steps (right heel strike to right toe off) in each load condition per participant. Data from each step were normalized to the maximum value of the processed signal observed during unloaded (0L) walking. Time-series signals were averaged for each muscle, for each load condition per participant.

Three walking simulations were developed for each condition per participant. Strides with clean, consecutive force plate strikes were selected from the 30-second recordings. Each walking simulation began at left mid-stance, contained one full stride, and ended at right mid-stance (approximately 1.5 strides total). Within each simulation, the portion of data between the first right heel strike and right toe off (right stance) was isolated for

Table 3. 1. Model muscle groups and their abbreviations. Individual muscles from the model that comprise the group as well as the total number of musculotendon actuators in each muscle group are given. Muscles corresponding to EMG signals are denoted with the superscript "E". Dominant (right) side muscles were evaluated.

Muscle group	Abbreviation	Individual muscles	# of musculotendon actuators
Paraspinals^{E}	ES	Multifidus and erector spinae: iliocostalis pars lumborum and longissimus pars lumborum	29
Obliques	OBL	External and internal obliques	12
Rectus abdominis	RA	Rectus abdominus	1
Psoas Major	PM	Psoas Major	11
Iliacus	IL	Iliacus	1
Gluteus Medius	GMED	Gluteus Medius, Gluteus Minimus	6
Gluteus Maximus	GMAX	Gluteus Maximus	3
Hamstrings	HAM	Semimembranosus, semitendinosus, biceps femoris long head	3
Rectus Femoris	RF	Rectus femoris	1
Vasti^{E}	VAS	Vastus lateralis, vastus intermedius, vastus medialis	3
Gastrocnemius^{E}	GAS	Gastrocnemius: medial and lateral heads	2
Soleus	SOL	Soleus	1

analysis because the left and right leg stance phases were assumed to be symmetric and it was expected for hip loads to be higher during stance compared to swing. Movement amplitude of the backpack relative to the torso in the global reference frame was extracted from the simulations as well as the segmental locations defined in Visual3D by marker positions. Individual muscles from the model were grouped based on anatomical location and function and their summed activations were extracted for analysis (Table 3. 1). Model muscle activations were low-pass filtered at 10 Hz and normalized to their peak activation during the unloaded condition for each person, and participant averages of activation time-series were computed for each load condition. Average activations estimated from static optimization were compared with EMG signals (Hicks et al., 2015). Three-dimensional L4-L5 and hip joint contact forces were low-pass filtered at 10 Hz and normalized by each participant's body weight (BW). Average joint contact forces during stance were compared in each coordinate direction, as well as peak forces in the axial and A/P directions. To interpret the joint contact force results, peak value and area under the curve (AUC) of processed EMG signals and muscle activations from the walking simulations were computed over stance and compared across walking conditions. Differences in outcome metrics between backpack load conditions were evaluated using repeated measures ANOVAs ($\alpha = 0.05$). We performed pairwise comparisons with Bonferroni corrections for multiple comparisons to evaluate differences between individual load conditions when significant main effects were found.

3.4 Results

Average self-selected walking speeds during experimental data collection were 1.575±0.212, 1.384±0.041, and 1.298±0.122 m/s for 0L, SHO, and HBA respectively.

3.4.1 Simulation Quality

Residual forces and moments from RRA (Table 3. 2) were generally low and similar across conditions with the largest root-mean-squared (RMS) force (FX: 1.096±0.872 %BW, or 9.157±6.710 N) and moment (MZ: 3.977±1.832 %BW-m, or 33.509±13.605 N-m) occurring during SHO. Kinematic tracking errors from RRA (Table 3. 3) were also low, and the largest RMS error in each condition was in pelvis tilt (0.632±0.687 deg, and 0.811±1.091 deg) during 0L and SHO respectively, and in trunk lateral bending (1.669±0.307 deg) during HBA. Average torso center-of-mass adjustments from RRA were less than 0.02 m in both the A/P and M/L directions for all load conditions. Simulated muscle activations compared well with experimental EMG measurements from GAS, VAS and ES in all conditions (Figure 3. 2). In general, ES simulated activations were greater than ES EMG especially during the loaded conditions.

Table 3. 2. Mean (standard deviation) RMS residual forces and moments from RRA applied to the pelvis during right side stance. Forces and moments were normalized to a percent of each participant's body weight (%BW) and then averaged for each walking condition.

	RMS Residual Forces (%BW)			RMS Residual Moments (%BW-m)		
	FX	FY	FZ	MX	MY	MZ
0L	0.530 (0.394)	0.833 (0.270)	0.537 (0.362)	3.175 (1.056)	2.695 (0.903)	2.739 (0.820)
SHO	1.096 (0.872)	0.590 (0.280)	0.239 (0.224)	2.235 (0.800)	3.490 (0.860)	3.977 (1.832)
HBA	0.805 (0.322)	0.770 (0.410)	0.517 (0.272)	2.726 (0.785)	2.968 (0.921)	2.428 (1.083)

Table 3. 3. Mean (standard deviation) of RMS and maximum kinematic tracking errors for each tracked model coordinate during RRA, averaged across participants for each load condition. All coordinates are in degrees except for pelvis mediolateral, anterior, and vertical translation, which are in meters.

	RMS tracking Error					
	0L		SHO		HBA	
	Translational Error (m)					
Pelvis mediolateral	0.013	(0.006)	0.011	(0.008)	0.018	(0.006)
Pelvis anterior	0.015	(0.008)	0.029	(0.018)	0.020	(0.008)
Pelvis vertical	0.025	(0.008)	0.023	(0.009)	0.025	(0.009)
	Rotational Error (deg)					
Pelvis tilt	0.632	(0.687)	0.811	(1.091)	0.156	(0.364)
Pelvis list	0.498	(0.550)	0.291	(0.435)	0.014	(0.028)
Pelvis rotation	0.062	(0.144)	0.028	(0.032)	0.024	(0.023)
Right hip flexion	0.309	(0.302)	0.660	(0.737)	0.340	(0.543)
Right hip adduction	0.009	(0.007)	0.028	(0.053)	0.012	(0.008)
Right hip rotation	0.025	(0.023)	0.020	(0.015)	0.010	(0.009)
Right knee angle	0.022	(0.035)	0.033	(0.031)	0.020	(0.020)
Right ankle angle	0.078	(0.047)	0.123	(0.101)	0.062	(0.107)
Left hip flexion	0.242	(0.410)	0.367	(0.520)	0.102	(0.179)
Left hip adduction	0.018	(0.013)	0.058	(0.169)	0.009	(0.004)
Left hip rotation	0.027	(0.025)	0.018	(0.017)	0.010	(0.008)
Left knee angle	0.039	(0.045)	0.046	(0.056)	0.045	(0.136)
Left ankle angle	0.067	(0.064)	0.107	(0.094)	0.027	(0.023)
Trunk extension	0.241	(0.765)	0.274	(0.488)	0.453	(0.233)
Trunk bending	0.060	(0.121)	0.079	(0.177)	1.669	(0.307)
Trunk rotation	0.030	(0.066)	0.055	(0.016)	0.085	(0.043)

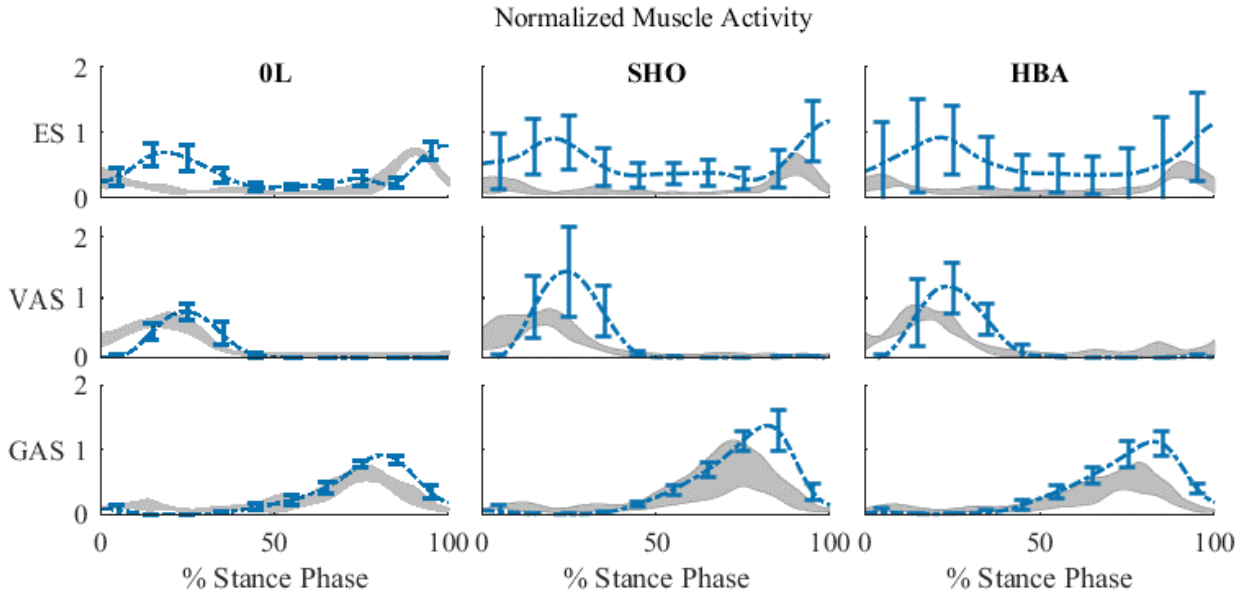

Figure 3. 2. Average processed electromyographic data (grey shaded region) and corresponding muscle activations from the walking simulations (blue dashed line with error bars) plotted over stance. Time-series data were normalized to the highest value observed during 0L for each muscle and subject.

Compared to experimentally determined backpack motion, average relative backpack motion in the vertical direction from walking simulations was 3.69x greater during SHO and 1.76x greater during HBA (Table 3. 4). Simulated backpack motion relative to the torso in the A/P direction was 0.383x the experimental amplitude during SHO. During HBA, A/P backpack motion from simulations was 0.941x the experimental amplitude. All average relative translations of the backpack from both the simulations and the experimentally tracked kinematic data were less than 5 cm. Backpack attachment parameter peak and average forces during walking were extracted from simulations for the SHO and HBA conditions (Table 3. 5). During HBA the vertical forces were distributed nearly evenly between the torso and pelvis attachments for both peak and average forces and they were approximately half the value of the respective vertical force at the torso attachment during SHO. Although the backpack attachment forces were not measured experimentally, these results are between measurements from an instrumented backpack with a rigid frame carrying 13.6 and 27.2 kg (LaFiandra and Harman, 2004). Average anterior/posterior force from the torso attachment was in opposite directions for the two pack conditions. During SHO, average A/P force was pushing the backpack load away from the torso; whereas, during HBA, this force was pulling the backpack load toward the torso. LaFiandra and Harman, 2004, using a hip-belt assisted backpack, found the average A/P force from the backpack COM to be approximately 0 N, but A/P forces between the upper(shoulder) and lower(pelvis) attachment points were nearly identical in magnitude and opposite in direction.

Table 3. 4. Relative amplitude of the motion between the backpack and the torso. The difference between the center-of-mass locations of the backpack and the torso in the global frame was extracted from simulations and 3D marker positions. Amplitudes were calculated as the range of this difference in the vertical and A/P directions. Results from all participants are averaged for both SHO and HBA.

	Amplitude of Backpack Movement (m)			
	Simulations		Experimental	
	Vertical	Anterior/Posterior	Vertical	Anterior/Posterior
SHO	0.0439	0.0106	0.0119	0.0277
HBA	0.0294	0.0174	0.0167	0.0185

Table 3. 5. Mean (standard deviation) of average and peak forces in the vertical and anterior/posterior directions reported from the backpack attachment parameters (spring and damper pairs) in N. Only torso attachment parameters are defined for the SHO model, while torso and pelvis attachment parameters are defined for the HBA model. Results from all participants are averaged for each load condition.

	Average Interaction Forces (N)			Peak Interaction Forces (N)		
	Torso_Vert	Torso_A/P	Pelvis_Vert	Torso_Vert	Torso_A/P	Pelvis_Vert
SHO	177.04 (8.81)	-35.77 (10.01)	N/A	283.46 (23.13)	-278.39 (90.52)	N/A
HBA	99.01 (11.16)	44.74 (39.25)	92.82 (10.92)	143.66 (12.63)	113.33 (40.54)	147.53 (11.41)

3.4.1 Joint Contact Forces

A significant main effect of backpack condition and post hoc pairwise comparisons were found for both average and peak joint contact forces (Table 3. 6). Carrying loads increased average axial L4-L5 force by 52.8%

(p=0.003) and 41.5% (p=0.022) during SHO and HBA compared to 0L respectively. Peak axial L4-L5 force was 51.2% greater (p=0.015) during SHO compared to 0L (Figure 3. 3). Peak and average hip axial force was approximately 30% greater during SHO (peak: p=0.020, average: p=0.011) and HBA (peak: p=0.008, average: p=0.031) compared to 0L (Figure 3. 3). Average hip A/P force was 34.1% (p=0.016) greater during SHO and 45.1% greater (p=0.022) during HBA compared to 0L. Peak hip A/P force was directed posteriorly and was approximately 30% greater during SHO (p=0.054) and HBA (p=0.050) (Figure 3. 3); however, SHO was not significantly different from 0L. No differences in joint contact forces were found between SHO and HBA.

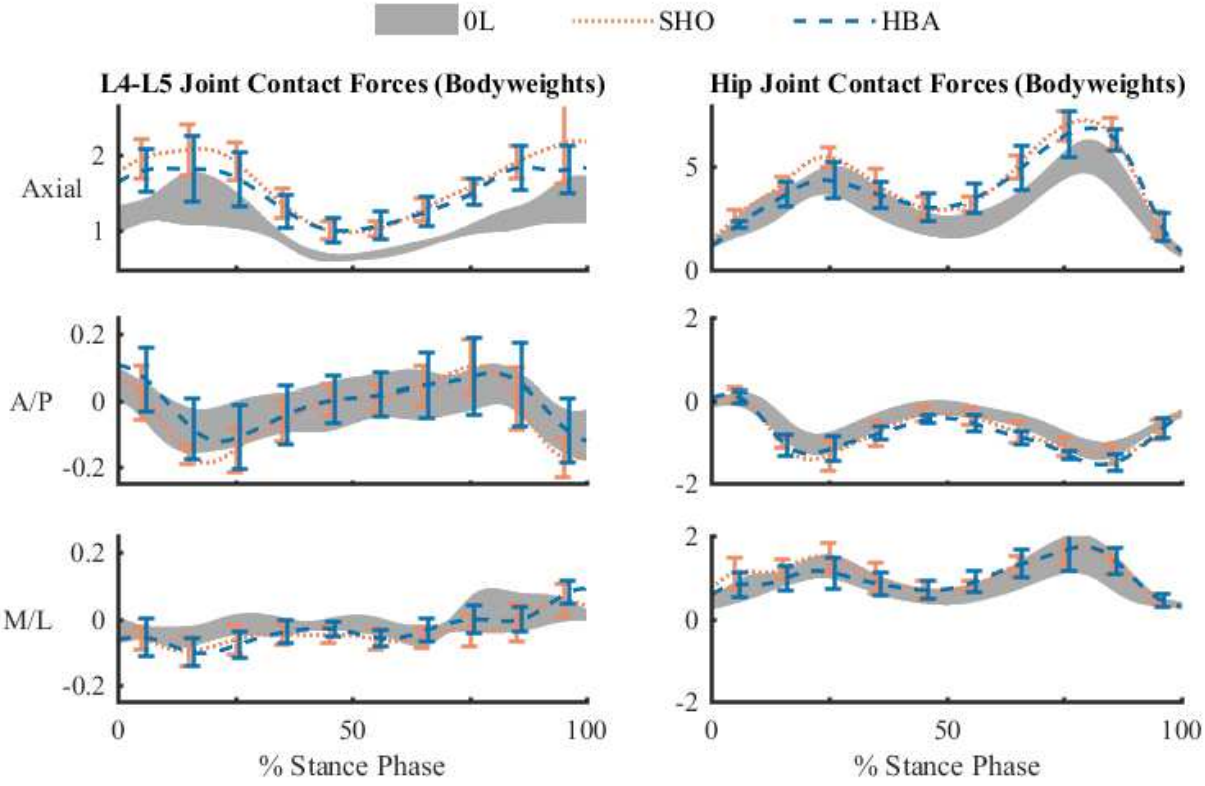

Figure 3. 3. Three-dimensional L4-L5 and Hip joint contact forces plotted over stance. 0L: grey shaded region representing the mean ± one standard deviation, SHO: orange dot-dashed line mean with vertical lines indicating ± one standard deviation, HBA: blue dashed line mean with vertical lines indicating ± one standard deviation. Forces were normalized to each participant's bodyweight and then averaged across participants. For L4-L5, the axial force is the compressive force between the two vertebrae, with the anterior and lateral (right side) directions defined positively. Hip joint contact forces between the pelvis and the femur are expressed in the femoral coordinate frame, with positive axial force being the compressive force along the direction of the femur, and anterior and lateral directions defined positively.

3.4.2 Muscle activity

From static optimization, only GAS model activation yielded a significant main effect for AUC (p=0.021), and post-hoc tests revealed that SHO was greater than 0L (p=0.005). This difference was attributed to the burst of GAS activity in the latter half of stance (Figure 3. 4). Main effects were found for peak model activations from static optimization in RF (p=0.048), BFSH (p=0.019), and GAS (p=0.028). Pairwise comparisons did not reveal any differences between individual conditions for peak RF activation, which was due to the conservative correction for

Table 3. 6. Main effects and pairwise comparison results for joint contact force metrics. p-values reported for main effects of backpack and pairwise comparisons between conditions are reported for average forces in L4-L5 and hip during stance (Top) and peak L4-L5 and hip forces during stance. Significant results are in bold.

	Main Effects		Pairwise Comparisons		
	F	P value	0L/SHO	0L/HBA	SHO/HBA
Average Joint Contact Force Results					
L4-L5 Axial	23.738	**0.000**	**0.003**	**0.022**	0.490
L4-L5 A/P	1.179	0.347			
L4-L5 M/L	2.170	0.165			
Hip Axial	9.958	**0.004**	**0.011**	**0.031**	1.000
Hip A/P	12.611	**0.002**	**0.016**	**0.022**	0.995
Hip M/L	1.662	0.238			
Peak Joint Contact Force Results					
L4-L5 Axial	11.031	**0.003**	**0.015**	0.065	0.533
L4-L5 A/P	3.760	0.061			
Hip Axial	11.280	**0.003**	**0.020**	**0.008**	1.000
Hip A/P	9.829	**0.004**	0.054	**0.050**	1.000

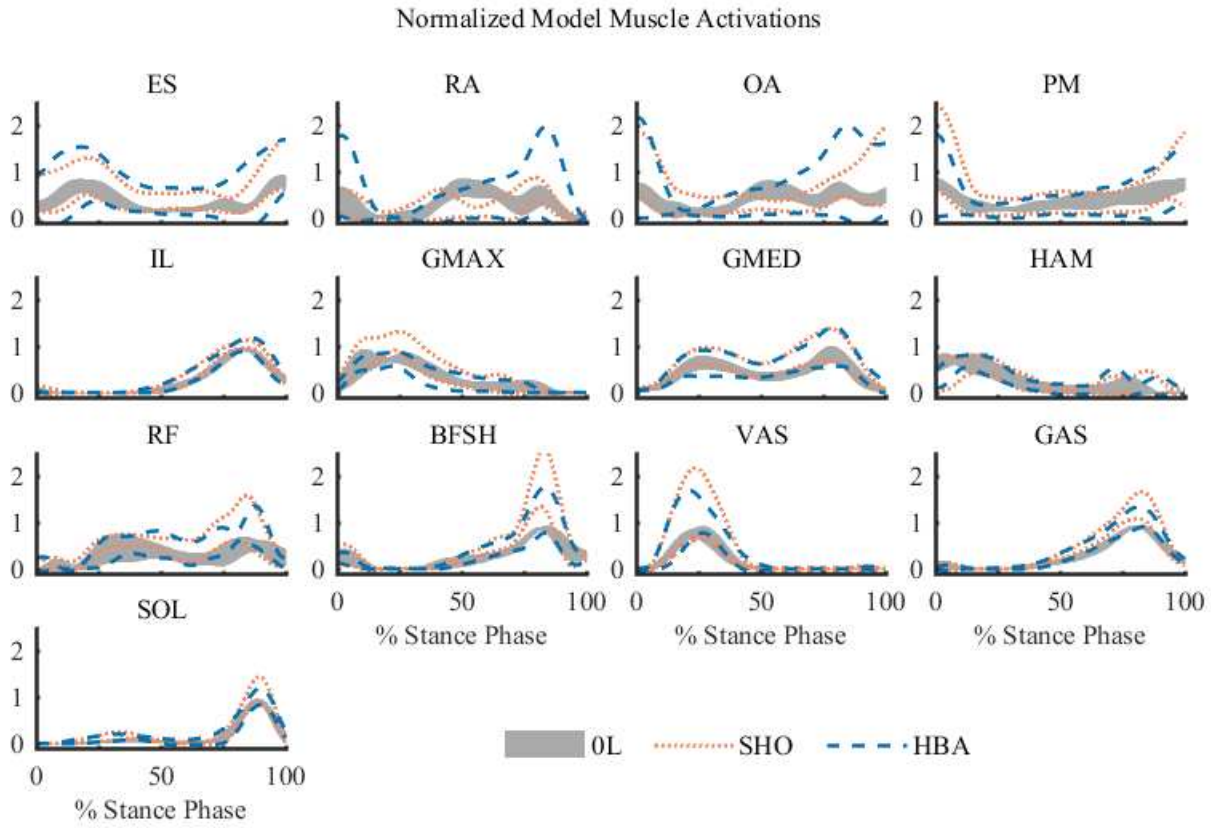

Figure 3. 4. Mean muscle activations (± 1 standard deviation) from static optimization over the stance phase for each walking condition averaged across participants. 0L – grey shaded region, SHO – orange dotted lines, HBA – blue dashed lines. Activations for each muscle were normalized to the highest value observed in 0L and averaged across participants.

multiple comparisons and large standard deviations as peak RF activation was 62% and 45% greater during SHO and HBA compared to 0L respectively. Peak BFSH and GAS activations were 127% (p=0.020) and 52% (p=0.029) greater during SHO than 0L respectively. In general, standard deviations of model activations from static optimization were greater during SHO and HBA than during 0L, and this increased variation was apparent in ES, RA, OBL, PM, and VAS (Figure 3. 4). Experimentally, for each EMG signal, there was one participant/condition in which the data were corrupt or non-salvageable due to artifact or noise. Therefore, the EMG signal from five participants was included for the statistical analysis of each experimentally measured muscle. One participant was removed for ES and another participant was removed from the analysis for GAS and VAS. A main effect for EMG metrics was found in peak ES^{EMG} activity (p=0.037), which was likely driven by lower values during SHO (0.619±0.159) and HBA (0.501±0.147) compared to 0L (0.788±0.044). However, pairwise comparisons for peak ES^{EMG} did not result in any significant differences between conditions, although HBA compared to 0L approached significance (p=0.078).

3.5 Discussion

The overall goal of this study was to quantify L4-L5 and hip joint contact forces during walking while unloaded and with different load carrying configurations. We achieved this by applying simulation techniques to a novel load carriage model. Residual forces and tracking errors from our simulations were low, and muscle activation patterns matched well with comparable EMG signals. Simulated ES had greater activation compared to EMG throughout stance during SHO and HBA, which may be due to passive muscle force properties that are not implemented during static optimization. Simulations resulted in a greater amplitude of vertical backpack motion and less A/P motion than was observed from the motion capture data during SHO, although translations were small (less than 5 cm on average). Backpack motion from simulations during HBA was generally similar to the motion capture data as the vertical range of backpack motion was greater, but A/P motion was nearly the same. These results indicate that the HBA model attachment parameters represented the corresponding physical backpack better than the SHO model did. Attachment parameters in the model could be tuned to replicate the motion amplitude from experimental data. However, it is difficult precisely measure the center of mass motion within a somewhat deformable backpack. In addition, the extent to which joint contact force estimates are influenced by the modeled attachment stiffness should be assessed through a parameter sensitivity analysis (see Chapter 4). Vertical backpack attachment forces were appropriate based on previous literature (LaFiandra and Harman, 2004) and distributed approximately equally between the pelvis and torso during the HBA condition. In addition, while vertical attachment forces at the pelvis and torso both acted to lift the backpack center of mass, average horizontal backpack forces were in opposite directions for the SHO and HBA conditions. During SHO, the horizontal attachment force was on average pushing the backpack away from the torso, which may be reflective of body contact that was not modeled. In the HBA condition, the average force was pulling the backpack toward the torso as may be expected when considering the nature of a physical backpack strap. This difference in behavior between SHO and HBA conditions may indicate an interaction between the shoulder and pelvis attachment points due to the model definition that results in keeping the backpack center-of-mass more posterior.

Our hypothesis that hip-belt assisted backpack condition would reduce lumbar joint contact forces compared to the shoulder-borne condition was not supported as both peak and average L4-L5 axial force was similar between HBA and SHO (peak: p=0.533, average: p=0.490) even though peak L4-L5 compressive force was 0.3 BW higher in SHO compared to HBA (Figure 3. 3). In addition, peak L4-L5 axial contact force during SHO was significantly greater than during 0L, while this force during HBA was not greater than 0L. However, peak L4-L5 axial force during HBA compared to 0L approached significance (p= 0.065), and this result should be further investigated in future studies with additional participants. The relative increases in average L4L5 axial force observed in this study (SHO: 52.8% and HBA: 41.5%) are similar to a 52.5% increase in intradiscal pressure measured during walking while carrying crates in both hands (Wilke et al., 2001, 1999). Recent work has observed that lower limb mechanical power and the relative contributions to this quantity from individual joints can be influenced by the design of load attachments (Lenton et al., 2018b), which suggests there may be differences in muscle force requirements as the joint power distribution is changed. However, we did not observe differences between SHO and HBA in activations of muscles spanning the hip joint such as GMAX, HAM, and RF. In addition, we found that hip joint contact forces increased by approximately 30% in both SHO and HBA compared to 0L, but were not different between the two backpack types. Therefore, our second hypothesis that hip-belt assisted designs would decrease hip joint contact forces and muscle activation in GMAX and HAM, while not affecting RF muscle activity was only partially supported because RF activity was similar between SHO and HBA.

While significant changes in muscle activations from the simulations were not observed except in GAS, the increases in joint contact forces are reflected by the collective increases in activation of muscle groups spanning each joint (Figure 3. 4). ES, OBL, and IL had greater AUC during both SHO and HBA compared to 0L to increase L4-L5 contact force. Likewise, greater activation in GMED and RF contributed to the larger hip joint contact forces during SHO and HBA compared to 0L. While not significant, GMAX and PM generated greater activation during SHO; whereas, these muscles had no change in activation between the HBA and 0L conditions. In addition, RA had less activation during SHO and greater activation during HBA relative to 0L. While a significant effect was detected in peak ES^{EMG}, pairwise comparisons did not confirm which individual conditions were different from each other. However, this conflicting result is likely due to a conservative correction for multiple comparisons as peak ES^{EMG} trended lower in both SHO and HBA compared to 0L. While ES, VAS, and GAS are important for load carriage, additional muscles should be measured to gain insight into the physiological demands of different types of backpacks in future work. Paraspinal and abdominal muscle activity as well as trunk posture varies with load placement in order to balance the different external moments from the added load (Bobet and Norman, 1984; Devroey et al., 2007; Goh et al., 1998). While individual muscle activations may be increased or decreased under specific loading configurations, the present findings suggest that the overall effect on joint contact forces remains unchanged. Therefore, the results of this study indicate that internal forces of the lower limb and lumbar spine are more greatly affected by the amount of load carried compared to backpack design.

The lack of a significant difference between SHO and HBA is likely due to the large standard deviation across participants. The participants had varying responses to the different designs, with three out of six participants having a peak L4-L5 load during SHO more than 0.3 BW greater than HBA, one participant having the opposite

relationship, and two participants whose peak L4L5 loads were very close in magnitude during both SHO and HBA. This variation is likely due to multiple factors including differences including variations in the self-selected walking speeds and the order of walking conditions (0L was always performed first, and the order of SHO and HBA was randomized). Walking speed significantly affects joint contact forces (Lenton et al., 2018a) and was not controlled in this study, which resulted in participants walking substantially slower overall in both SHO and HBA compared to 0L. This reduction in speed may be a strategy to mitigate peak joint loads and reduce metabolic cost. As a group, participants walked faster during SHO (1.38 m/s) than during HBA (1.30 m/s), but this relationship was not consistent across people and may be due to the order of walking conditions. Two participants had walking speeds during SHO that were within 0.02 m/s of their HBA average speed, and one participant walked almost 0.1 m/s faster during HBA than SHO. In addition, participants walked a total of 10 miles over the duration of the testing session, and fatigue may have affected the later conditions. It is possible that participants walked slower during HBA due to some restriction of motion imposed by the hip belt, and future studies should evaluate both stance and swing phase to investigate this effect. Future studies should further explore the effects of walking speed and incorporate a larger sample size given the large variation observed across participants. However, joint contact forces are expected to increase with walking speed. In the present study, participants walked 0.08 m/s slower and axial L4-L5 force was 0.3 BW lower during HBA compared to SHO. Therefore, while controlling walking speed for all conditions may reduce the deviations and increase the difference between loaded and unloaded conditions, we expect that the already small differences between HBA and SHO for L4-L5 contact forces will be further reduced. In addition, controlling walking speed may help elucidate whether these small differences between loading conditions are meaningful.

3.6 Conclusions

We successfully implemented a musculoskeletal model of backpack load carriage that distributed the total amount of load between the torso and pelvis based on attachment parameter definition in order to estimate joint contact forces. Key findings from this work suggests that backpack design may not be as influential to musculoskeletal injury risk during walking as the magnitude of load carried. However, small, but potentially meaningful, differences between backpack designs may have been undetected due to large standard deviations. Additional studies investigating joint contact forces and muscle activity during load carriage are warranted to address some of the limitations of the present work and facilitate model improvements. For example, a fixed walking speed or speeds should be controlled across load configurations for all participants as it can influence muscle activity and joint contact forces. In addition, electromyography from additional abdominal and hip muscles is important for further validation of the model implementation to ensure that the model responds appropriately to the external moment from the backpack. In the present work, only stance phase was analyzed as lower limb joint loads are greatest during this region. However, hip joint power may be affected by a hip-belt implementation during swing phase (Lenton et al., 2018b) and future analyses should focus on the complete gait cycle.

CHAPTER 4

EVALUATION OF BACKPACK ATTACHMENT PARAMETER UNCERTAINTY ON ESTMATES OF HIP AND LUMBAR SPINE JOINT CONTACT FORCE

4.1 Introduction

Backpack dynamics likely influence spinal loads, as they produce reaction forces at their points of attachment to the body (LaFiandra and Harman, 2004). Relative motion between the backpack and torso are influenced by the stiffness and damping properties of attachments (Ackerman et al., 2017; Foissac et al., 2009), and these properties will determine the reaction forces between backpack and body (Ren et al., 2005). The effective stiffness and damping of backpack attachments (i.e. shoulder straps and hip belts) is greatly influenced by factors other than the material properties of the backpack (Foissac et al., 2009). Therefore, parameter estimation for backpack attachment stiffness in a musculoskeletal model is difficult as parameters may be non-linear, there are multiple points of attachment to the body, and soft tissue interactions or individual participant differences will change effective stiffness of the link. In addition, it is unknown to what extent this uncertainty affects estimates of internal quantities such as joint contact and muscle forces.

Therefore, we performed a probabilistic sensitivity analysis to quantify the effect of backpack attachment parameter uncertainty on L4-L5 and hip contact force, and paraspinal and abdominal muscle activation. This analysis provided a measure of model robustness, indicating the level of confidence in the outcome metrics when the exact attachment parameters are uncertain.

4.2 Methods

Kinematic and kinetic data of a single walking trial each from two participants (P1: 31 years, 1.78 m, 86.64 kg; P2: 27 years, 1.83 m. 85.73 kg) while walking with a hip-belt assisted backpack load were used to drive musculoskeletal simulations using the methods previously described in Chapter 3. Stiffness and damping coefficient values for the hip-belt assisted backpack attachment definition were modeled as probability distributions and were varied within 1000 Monte-Carlo trials. Randomly selected parameter values were used to define linear spring and damper pairs attaching a backpack body to the torso and pelvis of a scaled and mass adjusted load carriage model (Chapter 3). A residual reduction algorithm was performed with the modified attachment parameters to create backpack motion; however, no additional mass or center-of-mass adjustments were performed.

Probability distributions were created for the stiffness and damping coefficients based on experimentally determined properties for a rigid backpack across a range of walking speeds (Foissac et al., 2009). Vertical (Vert) attachments to the torso and pelvis and an anterior/posterior (A/P) attachment to the torso were given identical distributions of stiffness (K) (Normal ~ 5060, ± 978 N m^{-1}) and damping (C) (Log-normal ~ 320 ± 125 N s m^{-1}). Outcome metrics calculated during each Monte-Carlo trial were peak hip and L4-L5 joint contact forces in the axial and A/P directions over the stance phase of walking. The absolute value was taken for each force so that a larger force corresponded to a greater positive value in each metric. A cumulative density function (CDF) was produced

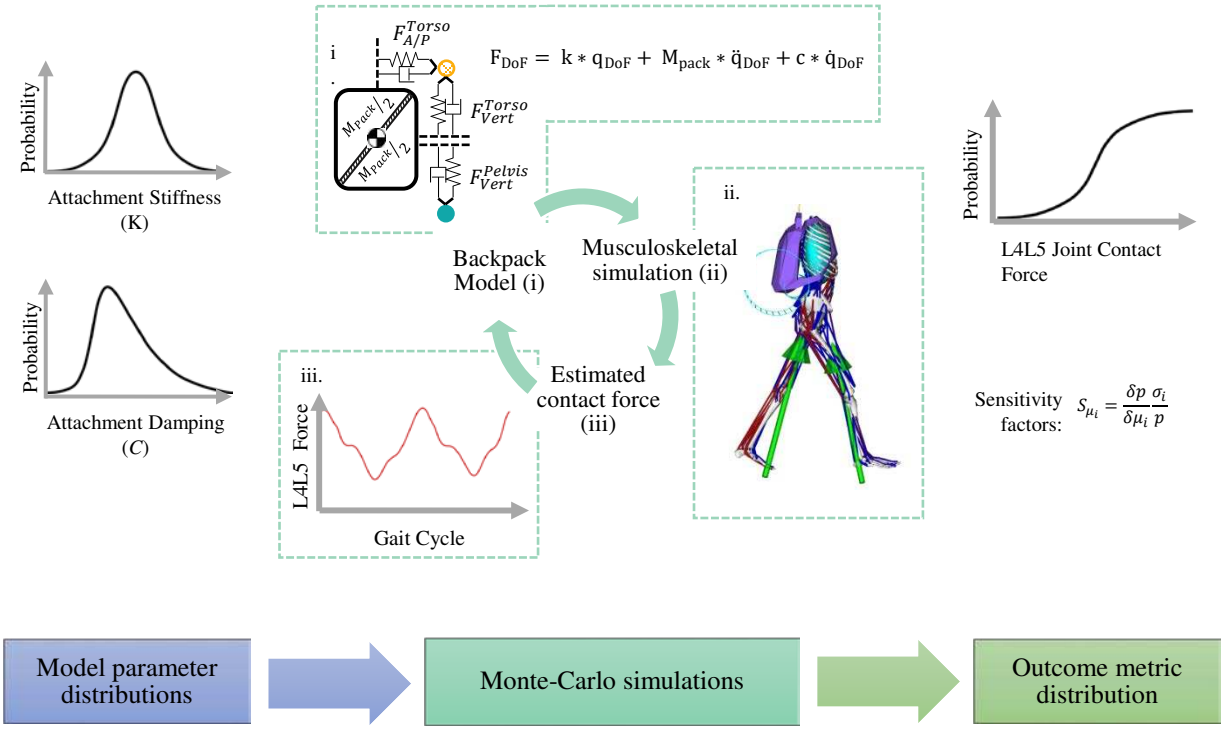

Figure 4. 1. Probabilistic analysis workflow. Backpack attachment parameter values are modeled as probability distributions. In a 1000 trial Monte-Carlo analysis, the backpack model is defined for each trial (i) using randomly selected values from the input distributions, then a musculoskeletal simulation is performed (ii) using this perturbed model and outcome metrics are extracted (iii) from each iteration to create a probability distribution of each outcome metric. This outcome distribution is then used to compute sensitivity factors attributed to each independent model parameter.

for each outcome metric which describes the value of the outcome metric at a given probability level (0 – 1). Coefficient of variation (COV) is the ratio of standard deviation relative to the mean as a percentage, and was computed for each outcome metric. Sensitivity factors were calculated to quantify the influence of the values of each independent backpack attachment parameter on each outcome metric (Equation 4. 1).

$$S_{\mu_i} = \frac{\delta p}{\delta \mu_i} \frac{\sigma_i}{p} \tag{4. 1}$$

where S_{μ_i} is the sensitivity factor for the mean of the outcome metric, p is the probability of the outcome metric and μ_i and σ_i are the mean and standard deviation of attachment parameter i. Positive sensitivity factors indicate a negative correlation between the outcome metric and the input parameter, which corresponds to an upward shift in the CDF of the outcome metric. Likewise, negative sensitivity factors indicate a positive correlation between the outcome metric and the input parameters. Sensitivity factors for the 0.1, 0.5, and 0.9 probability levels were output for each outcome metric and were averaged across the two participants.

4.3 Results

Results from both participants were similar, and the average values across both participants are reported for each metric. L4-L5 forces were more greatly influenced by changes in parameter values compared to hip forces.

COV for L4-L5 A/P force was 2.853%, and COV for L4-L5 axial force was 1.038%. Neither axial nor A/P forces in the hip were affected substantially with COV of 0.033% and 0.097% respectively. CFDs were centered at the mean for each outcome metric (L4-L5 Axial: 1615.05 N, L4-L5 A/P: 151.75 N, Hip Axial: 6719.03 N, Hip A/P: 1507.13 N) in order to compare visually (Figure 4. 2). The CDF for L4-L5 axial force was spread approximately 60 N (3.72% of the mean value) from the 0.05 to 0.95 probability levels, which was the widest distribution of outcome force (Figure 4. 2). The CDF width for L4-L5 A/P was the second widest at approximately 15 N (9.88% of mean value) even though it was by far the smallest outcome metric in magnitude. CDFs for the axial and A/P hip forces were less than 8 N (< 0.4% of mean values) wide. Sensitivity factors showed that both axial and A/P L4-L5 forces were influenced most by the vertical stiffness (K_{Vert}) parameters of the backpack-torso and backpack-pelvis attachments (Table 4. 1). Torso K_{Vert} and pelvis K_{Vert} had opposite effects on outcome metrics with $S_{\mu_{\text{Torso KVert}}} = -1.171(1.032)$ and $S_{\mu_{\text{Pelvis KVert}}} = 0.802(-1.087)$ for L4-L5 axial(A/P) averaged over the entire distribution (Table 4. 1). Hip A/P force was also most influenced by torso K_{Vert} ($S_{\mu_{\text{Torso KVert}}} = -0.842$) and pelvis K_{Vert} ($S_{\mu_{\text{Pelvis KVert}}} = 0.956$). However, hip axial force was most influenced by changes in vertical damping (C_{Vert}) of the backpack-pelvis attachment with $S_{\mu_{\text{Pelvis CVert}}} = 0.799$.

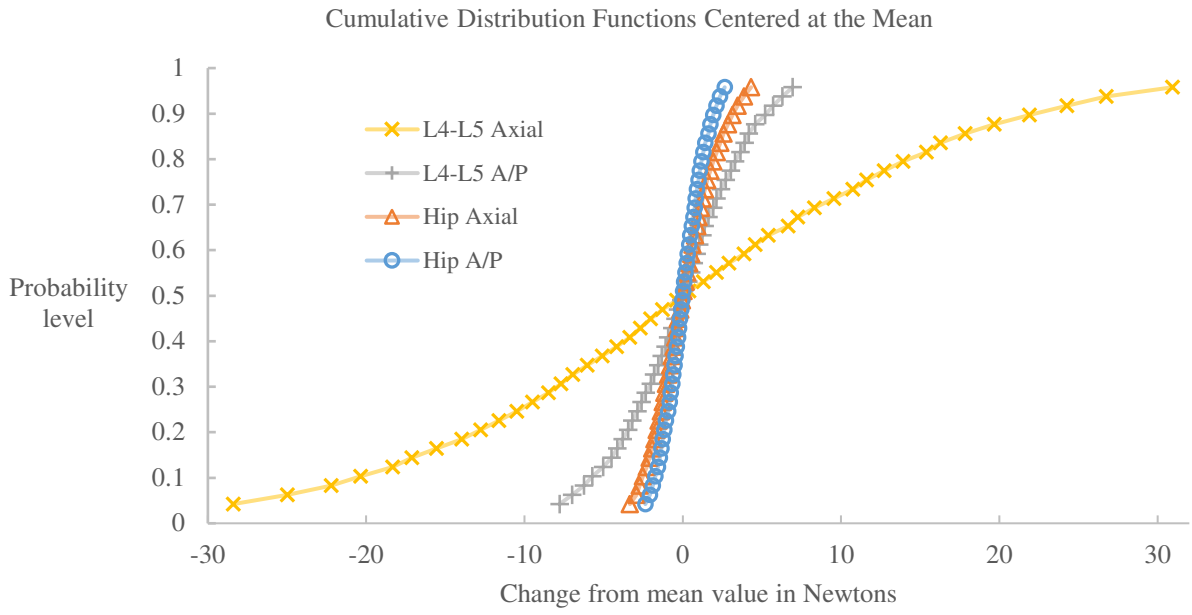

Figure 4. 2. Cumulative distribution functions (CDF's) of each joint contact force outcome. The baseline value (p=0.5 level) was subtracted from each CDF to center them at 0 and to represent the deviation from baseline rather than overall value of each metric.

Table 4. 1. Sensitivity factors for the mean value of each probabilistic model parameter at outcome probability levels 0.1, 0.5, and 0.9 as well as the average sensitivity factor from the entire distribution. Parameters with the greatest influence on

Outcome metric	Probability Level	Torso K_{AP}	Torso C_{AP}	Torso K_{Vert}	Torso C_{Vert}	Pelvis K_{Vert}	Pelvis C_{Vert}
L4-L5 Axial	0.1	0.028	0.141	**-1.444**	-0.282	0.693	0.207
	0.5	0.020	0.009	**-0.629**	-0.062	0.409	0.142
	0.9	0.123	0.182	**-1.209**	-0.127	1.110	0.141
	average	0.086	0.129	**-1.171**	-0.150	0.802	0.188
L4-L5 A/P	0.1	-0.002	-0.294	1.009	-0.136	**-1.444**	0.143
	0.5	0.080	-0.053	**0.575**	-0.058	-0.529	0.116
	0.9	0.187	-0.259	**1.334**	-0.039	-0.993	0.336
	average	0.073	-0.198	1.032	-0.080	**-1.087**	0.220
Hip Axial	0.1	-0.216	-0.357	-0.403	0.387	-0.069	**0.808**
	0.5	-0.017	-0.118	-0.106	0.129	-0.007	**0.455**
	0.9	-0.078	-0.217	-0.340	0.303	0.253	**0.925**
	average	-0.140	-0.257	-0.311	0.296	0.048	**0.799**
Hip A/P	0.1	0.168	0.294	**-1.113**	-0.928	0.848	0.009
	0.5	0.197	0.149	-0.365	-0.405	**0.490**	0.012
	0.9	0.334	0.249	-0.851	-0.639	**1.235**	0.068
	average	0.228	0.262	-0.832	-0.698	**0.956**	0.112

4.4 Discussion

The purpose of this study was to determine the effect of model parameter uncertainty L4-L5 and hip joint contact forces through a probabilistic analysis. L4-L5 axial force was the most sensitive to parameter uncertainty with a CDF width of 60 N; however, COV for L4-L5 axial force was only 1.038% indicating a small difference relative to the mean. L4-L5 A/P force had the largest COV of 2.853%, while neither axial or A/P hip forces had a COV greater than 0.01%. These relatively small variations indicate that L4-L5 and hip joint contact forces are not greatly affected by changes in attachment parameter values. L4-L5 axial force $S_{\mu_{\text{Torso KVert}}}$ was negative and $S_{\mu_{\text{Pelvis Kvert}}}$ was positive at all probability levels, which indicates that increased stiffness of the torso and pelvis attachment parameters increases and decreases L4-L5 axial (compressive) force, respectively. Increased stiffness of the torso vertical attachment parameter increased L4-L5 A/P force, while increased stiffness of the pelvis vertical attachment parameter decreased L4-L5 A/P force. This likely indicates that at the high end of the L4-L5 force distributions, the torso attachment parameter was at the upper range of stiffness and the pelvis attachment parameter was at the lower range of stiffness. In general sensitivity factors were had a v-shaped (or inverted v-shaped) pattern across the outcome distribution as they were larger near the tails (p = 0.1 and 0.9) of the distribution compared to the middle (p = 0.5). This effect was not as pronounced in $S_{\mu_{\text{Pelvis KVert}}}$ for L4-L5 axial force which was larger at the top

of the distribution (p = 0.9) than at the middle or the bottom. These patterns, combined with the opposing effects of torso K_{Vert} and pelvis K_{Vert}, suggest that changes parameter values have greater effect onL4-L5 axial and A/P force when the parameter values were defined at opposite ends of the input distributions.

A limitation of this analysis is that the backpack attachment parameter distributions defined in this study were estimated from a backpack with a mass rigidly fixed to a metal frame which was then attached to the body with shoulder and hip straps (Foissac et al., 2009). These parameters may be different from the backpacks used during the experimental data collection for the present analysis (see Chapter 3), and the outcome sensitivity to other parameter distributions should be investigated. However, the modeled uncertainties resulted in narrow probability distributions of all outcome forces. Therefore, while it is important to understand the approximate stiffness and damping of the backpacks to be modeled, precise definition of backpack attachment parameters may not be necessary for estimation of L4-L5 and hip joint contact force. This result is important for future load carriage modeling work as precise quantification of attachment stiffness and damping coefficients that incorporates the variable interaction between backpack straps and the person is difficult, and is likely not necessary to perform with high certainty.

4.4 Conclusion

Variation in L4-L5 joint contact forces was present due to the uncertainty modeled in the backpack attachment parameters. Outcome sensitivity was primarily driven by the uncertainty in the vertical stiffness parameters between the backpack and torso and the backpack and pelvis. The opposing interactions of torso and pelvis attachment definitions may be informative to equipment design, as the influence of parameter values on L4-L5 forces tended to increase at the tails of the outcome probability. However, the variation in L4-L5 force was low compared to the average force. Further analyses are warranted to investigate whether outcome metrics sensitivities are similarly affected by different attachment parameter distributions.

CHAPTER 5
SUMMARY AND CONCLUSIONS

The purpose of this work was to investigate the effects of backpack load distribution on the internal forces of the lumbar spine and the hip joints. In pursuit of this goal, a musculoskeletal model that incorporated a backpack with attachments to the torso and pelvis parameterized by spring and damper forces. Load carriage simulations were developed with this model using level walking data of US Marines using a shoulder-borne and a hip-belt assisted backpack. While joint contact forces in the lumbar spine and the hip were greater while carrying heavy loads compared to unloaded walking, there were no significant differences between the modeled backpack designs for any outcome metrics. Muscle activations were similar across all conditions, loaded and unloaded; however, there were large standard deviations in activation patters, which were likely due to variations in self-selected walking speed between participants and walking conditions. In addition, backpack attachment parameter definitions better represented the physical backpack in the hip-belt assisted design compared to the shoulder-borne design. To quantify the effect of this parameter uncertainty on estimates of joint contact forces at L4-L5 and at the hip, a sensitivity analysis was performed on the hip-belt assisted model using a 1000 trial Monte-Carlo approach. Lumbar joint contact forces were only slightly influenced and hip joint contact forces were relatively unaffected by the assumed uncertainty in the attachment parameter values. These overall findings suggest that backpack attachment parameters may not substantially influence joint contact forces in the lumbar spine and hips while walking on level ground. Rather, these forces are likely driven by the magnitude and position of carried load and walking speed. However, effective stiffness and damping of backpack attachments can be influenced by the how the wearer fastens the straps. Refinement of attachment parameters for each individual participant's model may slightly improve the accuracy of joint contact force estimates.

Walking on sloped surfaces causes postural and kinematic changes and increases mechanical demands on the body similar to load carriage, and are frequently encountered by service members carrying backpack loads. While the present work focused on load carriage on level ground, the interaction between load carriage and sloped walking surfaces should be investigated in future work. The combined postural responses to carrying backpack loads on inclined and declined surfaces may elicit differences between hip-belt assisted and shoulder-borne backpack designs. In addition, future work should control walking speed during experimental data collection in order to reduce variability in joint contact forces and muscle activations. Abdominal muscle activity was not measured experimentally, but it is important in understanding how the body acts to stabilize and accelerate the torso. Further validation of the musculoskeletal model used in this study should be performed incorporating electromyography from abdominal as well as hip extensor and flexor muscles in addition to the paraspinals and knee extensors evaluated in this work.

REFERENCES

Ackerman, J., Potwar, K., Seipel, J., 2017. Suspending loads decreases load stability but may slightly improve body stability. J. Biomech. 52, 38–47. https://doi.org/10.1016/j.jbiomech.2016.12.001

Actis, J.A., Honegger, J.D., Gates, D.H., Petrella, A.J., Nolasco, L.A., Silverman, A.K., 2018a. Validation of lumbar spine loading from a musculoskeletal model including the lower limbs and lumbar spine. J. Biomech. 68, 107–114. https://doi.org/10.1016/j.jbiomech.2017.12.001

Actis, J.A., Nolasco, L.A., Gates, D.H., Silverman, A.K., 2018b. Lumbar loads and trunk kinematics in people with a transtibial amputation during sit-to-stand. J. Biomech. 69, 1–9. https://doi.org/10.1016/j.jbiomech.2017.12.030

Anderson, F.C., Pandy, M.G., 2001a. Static and dynamic optimization solutions for gait are practically equivalent. J. Biomech. 34, 153–161. https://doi.org/10.1016/S0021-9290(00)00155-X

Anderson, F.C., Pandy, M.G., 2001b. Dynamic Optimization of Human Walking. J. Biomech. Eng. 123, 381. https://doi.org/10.1115/1.1392310

Anderson, F.C., Pandy, M.G., 1999. A Dynamic Optimization Soloution for Vertical Jumping in Three Dimensions. Comput. Methods Biomech. Biomed. Engin. 2, 201–231.

Armed Forces Health Surveillance Branch, 2017. Absolute and relative morbidity burdens attributable to various illnesses and injuries, active component, U.S. Armed Forces, 2016. MSMR 24, 2–8.

Attwells, R.L., Birrell, S.A., Hooper, R.H., Mansfield, N.J., 2006. Influence of carrying heavy loads on soldiers' posture, movements and gait. Ergonomics 49, 1527–1537. https://doi.org/10.1080/00140130600757237

Bachkosky, J., Andrews, M., Douglass, R., Feigley, J., Felton, L., Fernandez, F., Fratarangelo, P., Johnson-Winegar, A., Kohn, R., Polmar, N., Rumpf, R., Sommerer, J., Williamson, W., 2007. Lightening the Load.

Bassani, T., Stucovitz, E., Qian, Z., Briguglio, M., Galbusera, F., 2017. Validation of the AnyBody full body musculoskeletal model in computing lumbar spine loads at L4L5 level. J. Biomech. 58, 89–96. https://doi.org/10.1016/j.jbiomech.2017.04.025

Belmont Jr., L.P.J., Goodman, C.G.P., Waterman, C.B., DeZee, L.K., Burks, C.R., Owens, M.B.D., 2010. Disease and Nonbattle Injuries Sustained by a U.S. Army Brigade Combat Team During Operation Iraqi Freedom. Mil. Med. 175, 469:476.

Bobet, J., Norman, R.W., 1984. Effects of load placement on back muscle activity in load carriage. Eur. J. Appl. Physiol. Occup. Physiol. 53, 71–75. https://doi.org/10.1007/BF00964693

Bruno, A.G., Bouxsein, M.L., Anderson, D.E., 2015. Development and Validation of a Musculoskeletal Model of the Fully Articulated Thoracolumbar Spine and Rib Cage. J. Biomech. Eng. 137, 081003. https://doi.org/10.1115/1.4030408

Christophy, M., Senan, N.A.F., Lotz, J.C., O'Reilly, O.M., 2012. A Musculoskeletal model for the lumbar spine. Biomech. Model. Mechanobiol. 11, 19–34. https://doi.org/10.1007/s10237-011-0290-6

Collins, T.D., Ghoussayni, S.N., Ewins, D.J., Kent, J.A., 2009. A six degrees-of-freedom marker set for gait analysis: Repeatability and comparison with a modified Helen Hayes set. Gait Posture 30, 173–180. https://doi.org/10.1016/j.gaitpost.2009.04.004

Correa, T.A., Pandy, M.G., 2011. A mass – length scaling law for modeling muscle strength in the lower limb. J. Biomech. 44, 2782–2789. https://doi.org/10.1016/j.jbiomech.2011.08.024

Delp, S.L., Anderson, F.C., Arnold, A.S., Loan, P., Habib, A., John, C.T., Guendelman, E., Thelen, D.G., 2007. OpenSim: Open-Source Software to Create and Analyze Dynamic Simulations of Movement. IEEE Trans. Biomed. Eng. 54, 1940–1950. https://doi.org/10.1109/TBME.2007.901024

Delp, S.L., Loan, J.P., Hoy, M.G., Zajac, F.E., Topp, E.L., Rosen, J.M., 1990. An Interactive Graphics-Based Model of the Lower Extremity to Study Orthopaedic Surgical Procedures. IEEE Trans. Biomed. Eng. https://doi.org/10.1109/10.102791

Devroey, C., Jonkers, I., de Becker, A., Lenaerts, G., Spaepen, A., 2007. Evaluation of the effect of backpack load and position during standing and walking using biomechanical, physiological and subjective measures. Ergonomics 50, 728–742. https://doi.org/10.1080/00140130701194850

Dorn, T.W., Wang, J.M., Hicks, J.L., Delp, S.L., 2015. Predictive simulation generates human adaptations during loaded and inclined walking. PLoS One 10. https://doi.org/10.1371/journal.pone.0121407

Foissac, M., Millet, G.Y., Geyssant, A., Freychat, P., Belli, A., 2009. Characterization of the mechanical properties of backpacks and their influence on the energetics of walking. J. Biomech. 42, 125–130. https://doi.org/10.1016/j.jbiomech.2008.10.012

Ghori, G.M.U., Luckwill, R.G., 1985. Responses of the lower limb to load carrying in walking man. Eur. J. Appl. Physiol. Occup. Physiol. 54, 145–150. https://doi.org/10.1007/BF02335921

Goh, J.H., Thambyah, A., Bose, K., 1998. Effects of varying backpack loads on peak forces in the lumbosacral spine during walking. Clin. Biomech. 13, s26–s31. https://doi.org/10.1016/S0268-0033(97)00071-5

Granata, K.P., Orishimo, K.F., 2001. Response of trunk muscle coactivation to changes in spinal stability. J. Biomech. 34, 1117–1123. https://doi.org/10.1016/S0021-9290(01)00081-1

Harman, E., Frykman, P., Pandorf, C., Tharion, W., Mello, R., Obusek, J., Kirk, J., 1999. Physiological, biomechanical, and maximal performance comparisons of soldiers carrying loads using U.S. Marine Corps Modular Lightweight Load-Carrying Equipment (MOLLE), and U.S. Army Modular Load System (MLS) prototypes, USARIEM Technical Report.

Harman, E., Han, K.H., Frykman, P., Pandorf, C., 2000. The effects of backpack weight on the biomechanics of load carriage, USARIEM Technical Report. Natick, MA 01760-5007. https://doi.org/ADP010487

Hauret, K.G., Jones, B.H., Bullock, S.H., Canham-Chervak, M., Canada, S., 2010. Musculoskeletal injuries: Description of an under-recognized injury problem among military personnel. Am. J. Prev. Med. https://doi.org/10.1016/j.amepre.2009.10.021

Hicks, J.L., Uchida, T.K., Seth, A., Rajagopal, A., Delp, S.L., 2015. Is My Model Good Enough? Best Practices for Verification and Validation of Musculoskeletal Models and Simulations of Movement. J. Biomech. Eng. 137, 020905. https://doi.org/10.1115/1.4029304

Hinrichs, R.N., Lallement, S.R., Nelson, R.C., 1982. An Investigation of the Inertial Properties of Backpacks Loaded in Various Configurations. Natick, MA 01760-5007.

Hodge, W.A., Fijan, R.S., Carlson, K.L., Burgess, R.G., Harris, W.H., Mann, R.W., 1986. Contact pressures in the human hip joint measured in vivio. Proc. Natl. Acad. Sci. U. S. A. 83, 2879–2883. https://doi.org/10.1073/pnas.83.9.2879

Knapik, J., Harman, E., Reynolds, K., 1996. Load carriage using packs: A review of physiological, biomechanical and medical aspects. Appl. Ergon. 27, 207–216. https://doi.org/10.1016/0003-6870(96)00013-0

Krupenevich, R., Rider, P., Domire, Z., DeVita, P., 2015. Males and Females Respond Similarly to Walking With a Standardized, Heavy Load. Mil. Med. 180, 994–1000. https://doi.org/10.7205/MILMED-D-14-00499

Kutzner, I., Heinlein, B., Graichen, F., Bender, A., Rohlmann, A., Halder, A., Beier, A., Bergmann, G., 2010. Loading of the knee joint during activities of daily living measured in vivo in five subjects. J. Biomech. 43, 2164–2173. https://doi.org/10.1016/j.jbiomech.2010.03.046

LaFiandra, M., Harman, E., 2004. The Distribution of Forces between the Upper and Lower Back during Load Carriage. Med. Sci. Sports Exerc. 36, 460–467. https://doi.org/10.1249/01.MSS.0000117113.77904.46

Lee, P.J., Rogers, E.L., Granata, K.P., 2006. Active trunk stiffness increases with co-contraction. J. Electromyogr. Kinesiol. 16, 51–57. https://doi.org/10.1016/j.jelekin.2005.06.006

Lenton, G.K., Bishop, P.J., Saxby, D.J., Doyle, T.L.A., Pizzolato, C., Billing, D., Lloyd, D.G., 2018a. Tibiofemoral joint contact forces increase with load magnitude and walking speed but remain almost unchanged with different types of carried load. PLoS One 13, 1–14. https://doi.org/10.1371/journal.pone.0206859

Lenton, G.K., Doyle, T.L.A., Lloyd, D.G., Higgs, J., Billing, D., Saxby, D.J., 2018b. Lower-limb joint work and

power are modulated during load carriage based on load configuration and walking speed. J. Biomech. 83, 174–180. https://doi.org/10.1016/j.jbiomech.2018.11.036

Lenton, G.K., Saxby, D.J., Lloyd, D.G., Billing, D., Higgs, J., Doyle, T.L.A., 2018c. Primarily hip-borne load carriage does not alter biomechanical risk factors for overuse injuries in soldiers. J. Sci. Med. Sport 22, 158–163. https://doi.org/10.1016/j.jsams.2018.06.013

Lu, T.W., O'Connor, J.J., 1999. Bone position estimation from skin marker co-ordinates using global optimisation with joint constraints. J. Biomech. 32, 129–134. https://doi.org/10.1016/S0021-9290(98)00158-4

Milgrom, C., 2001. The role of strain and strain rates in stress fractures., in: Burr, D.B., Milgrom, C. (Eds.), Musculoskeletal Fatigue and Stress Fractures. Lewis publisher, Boca Raton, FL, p. 332. https://doi.org/10.1016/S1353-8020(08)70020-8

Muslim, K., Nussbaum, M.A., 2016a. Traditional posterior load carriage: effects of load mass and size on torso kinematics, kinetics, muscle activity and movement stability. Ergonomics 59, 99–111. https://doi.org/10.1080/00140139.2015.1053538

Muslim, K., Nussbaum, M.A., 2016b. Traditional posterior load carriage effects of load mass and size on torso kinematics kinetics muscle activity and movement stability. Ergonomics 59, 99–111. https://doi.org/10.1080/00140139.2015.1053538

Neptune, R.R., Sasaki, K., Kautz, S.A., 2008. The effect of walking speed on muscle function and mechanical energetics. Gait Posture 28, 135–143. https://doi.org/10.1016/j.gaitpost.2007.11.004

Paul, S., Bhattacharyya, D., Chatterjee, T., Majumdar, D., 2016. Effect of uphill walking with varying grade and speed during load carriage on muscle activity. Ergonomics 59, 514–525. https://doi.org/10.1080/00140139.2015.1073792

Pelot, R.P., Rigby, A., Stevenson, J.M., Bryant, J.T., 2000. Defense Technical Information Center Compilation Part Notice TITLE: A Static Biomechanical Load Carriage Model TITLE: Soldier Mobility: Innovations in Load Carriage System Design and Evaluation [la Mobilite du combattant: innovations dans la conception et. Proc. NATO RTO Meet. 56 Innov. Load Carriage Syst. Des. Eval. Kingston, Canada.

Piazza, S.J., 2006. Muscle-driven forward dynamic simulations for the study of normal and pathological gait. J. Neuroeng. Rehabil. 3, 1–7. https://doi.org/10.1186/1743-0003-3-5

Raabe, M.E., Chaudhari, A.M.W., 2016. An investigation of jogging biomechanics using the full-body lumbar spine model : Model development and validation. J. Biomech. 49, 1238–1243. https://doi.org/10.1016/j.jbiomech.2016.02.046

Rajagopal, A., Dembia, C., DeMers, M., Delp, D., Hicks, J., Delp, S., 2016. Full body musculoskeletal model for muscle- driven simulation of human gait. IEEE Trans. Biomed. Eng. 63, 2068–2079. https://doi.org/10.1109/TBME.2016.2586891

Ramsay, J.W., Hancock, C.L., O'Donovan, M.P., Brown, T.N., 2016. Soldier-relevant body borne loads increase knee joint contact force during a run-to-stop maneuver. J. Biomech. 49, 3868–3874. https://doi.org/10.1016/j.jbiomech.2016.10.022

Ren, L., Jones, R.K., Howard, D., 2005. Dynamic analysis of load carriage biomechanics during level walking. J. Biomech. 38, 853–863. https://doi.org/10.1016/j.jbiomech.2004.04.030

Sasaki, K., Neptune, R.R., 2010. Individual muscle contributions to the axial knee joint contact force during normal walking. J. Biomech. 43, 2780–2784. https://doi.org/10.1016/j.jbiomech.2010.06.011

Schache, A.G., Kim, H.J., Morgan, D.L., Pandy, M.G., 2010. Hamstring muscle forces prior to and immediately following an acute sprinting-related muscle strain injury. Gait Posture 32, 136–140. https://doi.org/10.1016/j.gaitpost.2010.03.006

Schuh, A., Grier, T., Canham-chervak, M., Schuh, A., Grier, T., Canham-, M., Hauschild, V., Roy, T., Jones, H., 2017. Public Health Report No . S . 0047785-17 , March 2017 Clinical Public Health and Epidemiology Injury Prevention Division Risk Factors for Injury Associated with Low , Moderate , and High Mileage Road Marching in a U . S . Army Infantry Brigade Prepared by. Aberdeen Proving Ground.

Schwartz, M.H., Rozumalski, A., 2005. A new method for estimating joint parameters from motion data. J. Biomech. 38, 107–116. https://doi.org/10.1016/j.jbiomech.2004.03.009

Seay, J.F., Fellin, R.E., Sauer, S.G., Frykman, P.N., Bensel, C.K., 2014. Lower Extremity Biomechanical Changes Associated With Symmetrical Torso Loading During Simulated Marching. Mil. Med. 179. https://doi.org/10.7205/MILMED-D-13-00090

Selk Ghafari, A., Meghdari, A., Vossoughi, G.R., 2010. Biomechanical analysis for the study of muscle contributions to support load carrying. Proc. Inst. Mech. Eng. Part C J. Mech. Eng. Sci. 224. https://doi.org/10.1243/09544062JMES1559

Silverman, A.K., Neptune, R.R., 2014. Three-dimensional knee joint contact forces during walking in unilateral transtibial amputees. J. Biomech. 47, 2556–2562. https://doi.org/10.1016/j.jbiomech.2014.06.006

Stevenson, J.M., Bossi, L.L., Bryant, J.T., Reid, S.A., Pelot, R.P., Morin, E.L., 2000. A suite of objective biomechanical measurement tools for personal load carriage system assessment, in: Proceedings of NATO RTO Meeting 56: Innovations in Load Carriage System Design and Evaluation, Kingston, Canada. https://doi.org/10.1080/00140130410001699119

Sutherland, D.H., 2001. The evolution of clinical gait analysis part 1: Kinesiological EMG. Gait Posture 14, 61–70. https://doi.org/10.1016/S0966-6362(01)00100-X

Tafazzol, A., Arjmand, N., Shirazi-Adl, A., Parnianpour, M., 2014. Lumbopelvic rhythm during forward and backward sagittal trunk rotations: Combined in vivo measurement with inertial tracking device and biomechanical modeling. Clin. Biomech. 29, 7–13. https://doi.org/10.1016/j.clinbiomech.2013.10.021

U.S. Army Public Health Center, 2017. Health Of The Force Report. https://doi.org/TA-419-0318

Wang, H., Frame, J., Ozimek, E., Leib, D., Dugan, E.L., 2013. The effects of load carriage and muscle fatigue on lower-extremity joint mechanics. Res. Q. Exerc. Sport 84. https://doi.org/10.1080/02701367.2013.814097

Wilke, H.-J., Neef, P., Caimi, M., Hoolgand, T., Claes, L.E., 1999. New In Vivo Measurements of Pressures in the Intervertebral Disc in Daily Life. Spine (Phila. Pa. 1976). 24, 755–762.

Wilke, H.-J., Neef, P., Hinz, B., Seidel, H., Claes, L., 2001. Intradiscal pressure together with anthropometric data – a data set for the validation of models. Clin. Biomech. 16, Supple, S111--S126. https://doi.org/10.1016/S0268-0033(00)00103-0

Yamaguchi, G.T., Zajac, F.E., 1989. A planar model of the knee joint to characterize the knee extensor mechanism. J. Biomech. 22, 1–10. https://doi.org/10.1016/0021-9290(89)90179-6

Yoder, A.J., Petrella, A.J., Silverman, A.K., 2015. Trunk-pelvis motion, joint loads, and muscle forces during walking with a transtibial amputation. Gait Posture 41, 757–762. https://doi.org/10.1016/j.gaitpost.2015.01.016

Zajac, F.E., 1989. Muscle and Tendon: Properties, models, scaling, and application to biomechanics and motor control. Crit. Rev. Biomed. Eng. 17, 359–411.

Zajac, F.E., Neptune, R.R., Kautz, S.A., 2003. Biomechanics and muscle coordination of human walking. Part II: Lessons from dynamical simulations and clinical implications. Gait Posture 17, 1–17.

Zajac, F.E., Neptune, R.R., Kautz, S.A., 2002. Biomechanics and muscle coordination of human walking. Part I: introduction to concepts, power transfer, dynamics and simulations. Gait Posture 16, 215–32.